

However, the pH remote loading method is not available for DXR encapsulation into the albumin-conjugated PEG liposome, since carbodiimide can activate carbonyl group only at a low pH region, especially between 3.5 and 4.5 during the first step of reaction (Nakajima and Ikada, 1995). Therefore, in the present study, we chose SPDP as the hetero-bifunctional-cross-linker (Carlsson et al., 1978) to prepare rHSA/PEG liposomes, because the coupling reaction can be conducted under weakly alkaline pH, which makes it possible to perform the pH remote loading method for encapsulating DXR into rHSA/PEG liposomes. SPDP has been widely used for the preparation of disulphide-linked protein–protein conjugates (Moll and Thompson, 1994; Takeoka et al., 2001) and immunoliposome (Barbet et al., 1981; Ishimori et al., 1984; Schwendener et al., 1990). As a result, the encapsulation efficiency of DXR into rHSA/PEG liposomes or PEG liposomes was very high and more than 95% of DXR added was successfully encapsulated.

In vivo disposition studies in tumor-bearing rats revealed that the DXR encapsulation into rHSA/PEG liposomes or PEG liposomes dramatically changed the in vivo disposition characteristics of DXR itself (Fig. 1 and Table 1). Furthermore, rHSA-conjugation onto the surface of liposomes significantly prolonged the blood circulation of DXR compared with PEG liposomal DXR. Taken that the in vitro release study demonstrated that DXR was stably and similarly encapsulated within both liposomal preparations in the presence of plasma and that free DXR was immediately cleared from the blood circulation after injection (Fig. 1), the in vivo disposition characteristics of rHSA/PEG liposomal DXR or PEG liposomal DXR is considered to mainly represent the pharmacokinetics of each PEG liposomes themselves. In addition, rHSA/PEG liposomes significantly reduced the hepatic and splenic clearances of DXR compared with PEG liposomes, although both PEG liposomal preparations remarkably decreased both tissue clearances compared with free DXR (Fig. 2B). Although the disposition amount of DXR in the liver and spleen was larger for both rHSA/PEG and PEG liposomal DXR than that for free DXR, it would be because the distribution of DXR into and the subsequent elimination of DXR from the liver is delayed and prolonged for liposomal preparations, compared with free DXR. The distribution of free DXR to and its subsequent elimination from the liver due to the metabolism, biliary excretion or efflux back to the blood stream are very fast (Colombo et al., 1994; Working and Dayan, 1996). In the case of heart, the amount of DXR at 3 h would reflect the accumulation of DXR in heart (Figs. 2 and 4), considering the very rapid elimination of free DXR from plasma (Fig. 1). Clearance values also confirmed that both PEG liposomal preparations significantly attenuated DXR distribution to heart (Fig. 2B). As Speth et al. (1988) reported that one of the acute or delayed toxicities derived from DXR was cardiac arrhythmias or cardiomyopathy, respectively, the decrease in DXR distribution to heart would be one of the advantages rHSA/PEG liposome can provide.

As described above, in vivo disposition studies clearly indicated the longer circulation of rHSA/PEG liposomal DXR and lower values of tissue clearances for liver and spleen than PEG liposomal DXR. The serum proteins associated onto the surface

of liposomes systematically administered have been suggested to be one of the most important factors to determine their in vivo fate (Drummond et al., 1999; Luigi et al., 2003). Chonn et al. (1992) reported that the amount of serum proteins associated on the liposomes used was inversely related to their circulation half-lives. Our present findings also revealed that less amount of serum proteins was associated on rHSA/PEG liposomes than PEG liposomes (Fig. 3). Since the recognition of surface-associated serum opsonins by their corresponding receptors is mainly a trigger for the receptor-mediated hepatic uptake of liposomes, it is considered that the rHSA-conjugation on PEG liposome suppressed the association of serum proteins including some serum opsonins. Western blotting will be useful to address the possible less-association of typical serum opsonins on rHSA/PEG liposome and will be the subject of our further study.

The movement of liposomes into the tumor interstitium is principally via extravasation through the discontinuous endothelium of the tumor microvasculature (Drummond et al., 1999). Since the maintenance of high blood level or large AUC of particulate drug carriers is one of the driving forces for the efficient extravasation into tumor tissues (Drummond et al., 1999), it can be considered that rHSA/PEG liposomal preparation successfully improved the tumor disposition of DXR over PEG liposomal preparation via EPR effect (Fig. 4). For DXR to exert the anti-tumor effect, DXR must be released and taken up by the surrounding tumor cells. Although DXR is stably incorporated in rHSA/PEG liposomes in plasma, DXR release from the liposome preparations would be enhanced after liposomes are extravasated into tumor tissues, considering that malignant effusions significantly elevated the release of DXR from liposome preparation (Gabizon, 1995). Elucidation of local release profile of DXR in tumor tissues will be the subject for further study.

From the viewpoint of clinical therapeutics, the balance between pharmacological and adverse effects is very important. Therefore, we calculated the therapeutic index defined as the ratio of the amount of DXR delivered to tumor, the site of action, to the DXR amount at potential sites of toxicity, heart (Fig. 4). Therapeutic index was the highest for rHSA/PEG liposomal DXR, suggesting that rHSA-conjugation on PEG liposome would increase the anti-tumor effect as well as the safety of liposomal DXR.

In conclusion, rHSA modification on the surface of PEG liposome significantly prolonged the blood circulation time of PEG liposomal DXR, leading to higher DXR amount in the tumor, but lower level of DXR in heart after intravenous administration. These findings are very useful to optimize albumin-conjugated PEG liposome for the passive targeting of encapsulated drug and for the better therapeutic outcome.

References

- Abraham, S.A., Waterhouse, D.N., Mayer, L.D., Cullis, P.R., Madden, T.D., Bally, M.B., 2005. The liposomal formulation of doxorubicin. *Methods Enzymol.* 391, 71–97.
- Allen, T.M., Hansen, C., Rutledge, J., 1989. Liposomes with prolonged circulation times: factors affecting uptake by reticuloendothelial and other tissues. *Biochim. Biophys. Acta* 981, 27–35.

- Allen, T.M., Hansen, C., Martin, F., Redemann, C., Yau-Young, A., 1991. Liposomes containing synthetic lipid derivatives of poly(ethylene glycol) show prolonged circulation half-lives in vivo. *Biochim. Biophys. Acta* 1066, 29–36.
- Bally, M.B., Nayar, R., Masin, D., Hope, M.J., Cullis, P.R., Mayer, L.D., 1990. Liposomes with entrapped doxorubicin exhibit extended blood residence times. *Biochim. Biophys. Acta* 1023, 133–139.
- Barbet, J., Machy, P., Leserman, L.D., 1981. Monoclonal antibody covalently coupled to liposomes: specific targeting to cells. *J. Supramol. Struct. Cell Biochem.* 16, 243–258.
- Blume, G., Cevc, G., 1990. Liposomes for the sustained drug release in vivo. *Biochim. Biophys. Acta* 1029, 91–97.
- Bolotin, E.M., Cohen, R., Bar, L.K., Emanuel, S.N., Lasic, D.D., Barenholz, Y., 1994. Ammonium sulfate gradients for efficient and stable remote loading of amphiphatic weak bases into liposomes and ligandliposomes. *J. Liposome Res.* 4, 455–479.
- Carlsson, J., Drevin, H., Axen, R., 1978. Protein thiolation and reversible protein-protein conjugation. *N-Succinimidyl 3-(2-pyridylidithio) propionate, a new heterobifunctional reagent.* *Biochem. J.* 173, 723–737.
- Chonn, A., Semple, S.C., Cullis, P.R., 1992. Association of blood proteins with large unilamellar liposomes in vivo: relation to circulation lifetimes. *J. Biol. Chem.* 267, 18759–18765.
- Colombo, T., Zucchetti, M., D'Incalci, M., 1994. Cyclosporin A markedly changes the distribution of doxorubicin in mice and rats. *J. Pharmacol. Exp. Ther.* 69, 22–27.
- Dilgimen, A.S., Mustafaeva, Z., Demchenko, M., Kaneko, T., Osada, Y., Mustafaeva, M., 2001. Water-soluble covalent conjugates of bovine serum albumin with anionic poly(*N*-isopropyl-acrylamide) and their immunogenicity. *Biomaterials* 22, 2383–2392.
- Dresdale, A., Bonow, R.O., Wesley, R., Palmeri, S.T., Barr, L., Mathison, D., D'Angelo, T., Rosenberg, S.A., 1983. Prospective evaluation of doxorubicin-induced cardiomyopathy resulting from postsurgical adjuvant treatment of patients with soft tissue sarcomas. *Cancer* 52, 51–60.
- Drummond, D.C., Meyer, O., Hong, K., Kirpotin, D.B., Papahadjopoulos, D., 1999. Optimizing liposomes for delivery of chemotherapeutic agents to solid tumors. *Pharmacol. Rev.* 51, 691–743.
- Embre, L., Gelmon, K.A., Lohr, A., Mayer, L.D., Coldman, A.J., Cullis, P.R., Palatis, W., Plikiewicz, F., Hudon, N.J., Heggie, J.R., Goldie, J.H., 1993. Chromatographic analysis and pharmacokinetics of liposome-encapsulated doxorubicin in non-small-cell lung cancer patients. *J. Pharm. Sci.* 82, 627–634.
- Endoh, H., Suzuki, Y., Hashimoto, Y., 1981. Antibody coating of liposomes with 1-ethyl-3-(3-dimethyl-aminopropyl)carbodiimide and the effect on target specificity. *J. Immunol. Methods* 44, 79–85.
- Furumoto, K., Yokoe, J., Ogawara, K., Amano, S., Takaguchi, M., Higaki, K., Kai, T., Kimura, T., 2007. Effect of coupling of albumin onto surface of PEG liposome on its in vivo disposition. *Int. J. Pharm.* 329, 110–116.
- Gabizon, A., Papahadjopoulos, D., 1992. The role of surface charge and hydrophilic groups on liposome clearance in vivo. *Biochim. Biophys. Acta* 1103, 94–100.
- Gabizon, A.A., Barenholz, Y., Bialer, M., 1993. Prolongation of the circulation time of doxorubicin encapsulated in liposomes containing a polyethylene glycol-derivatized phospholipid: pharmacokinetic studies in rodents and dogs. *Pharm. Res.* 10, 703–708.
- Gabizon, A.A., 1995. Liposome circulation time and tumor targeting: implications for cancer chemotherapy. *Adv. Drug Deliv. Rev.* 16, 285–294.
- Gabizon, A., Shmeeda, H., Barenholz, Y., 2003. Pharmacokinetics of pegylated liposomal doxorubicin: review of animal and human studies. *Clin. Pharmacokinet.* 42, 419–436.
- Harashima, H., Kiwada, H., 1996. Liposomal targeting and drug delivery: kinetic consideration. *Adv. Drug Deliv. Rev.* 19, 425–444.
- Harashima, H., Ishida, T., Kamiya, H., Kiwada, H., 2002. Pharmacokinetic of targeting with liposomes. *Crit. Rev. Ther. Drug Carrier Syst.* 19, 235–275.
- Ishimori, Y., Yasuda, T., Tsumita, T., Notsuki, M., Koyama, M., Tadokuma, T., 1984. Liposome immune lysis assay (LILA): a simple method to measure anti-protein antibody using protein antigen-bearing liposomes. *J. Immunol. Methods* 75, 351–360.
- Jang, S.H., Wientjes, M.G., Lu, D., Au, J.L.S., 2003. Drug delivery and transport to solid tumors. *Pharm. Res.* 20, 1337–1350.
- Klibanov, A.L., Maruyama, K., Torchilin, V.P., Huang, L., 1990. Amphiphatic polyethyleneglycols effectively prolong the circulation time of liposomes. *FEBS Lett.* 268, 235–237.
- Lowry, O.H., Rosebrough, N.J., Farr, A.L., Randall, R.J., 1951. Protein measurement with the Folin phenol reagent. *J. Biol. Chem.* 193, 265–275.
- Luigi, C., Maurizio, C., Franco, D., 2003. From conventional to stealth liposomes. A new frontier in cancer chemotherapy. *Tumori* 89, 237–249.
- MacAdam, A.B., Shafiq, Z.B., Marriott, C., Martin, G.P., James, S.L., 2000. Anti-mucus polyclonal antibody production, purification and linkage to the surface of albumin microspheres. *Int. J. Pharm.* 195, 147–158.
- Madden, T.D., Harrigan, P.R., Tai, L.C., Bally, M.B., Mayer, L.D., Redelmeier, T.E., Loughrey, H.C., Tilcock, C.P., Reinisch, L.W., Cullis, P.R., 1990. The accumulation of drugs within large unilamellar vesicles exhibiting a proton gradient: a survey. *Chem. Phys. Lipids* 53, 37–46.
- Maeda, H., Wu, J., Sawa, T., Matsumura, Y., Hori, K., 2000. Tumor vascular permeability and the EPR effect in macromolecular therapeutics. *J. Control. Release* 65, 271–284.
- Maruyama, K., Yuda, T., Okamoto, A., Kojima, S., Sugiyama, A., Iwatsuru, M., 1992. Prolonged circulation time in vivo of large unilamellar liposomes composed of distearoyl phosphatidylcholine and cholesterol containing amphiphatic poly(ethylene glycol). *Biochim. Biophys. Acta* 1128, 44–49.
- Mayer, L.D., Bally, M.B., Cullis, P.R., 1986. Uptake of adriamycin into large unilamellar vesicles in response to a pH gradient. *Biochim. Biophys. Acta* 857, 123–126.
- Moll, T.S., Thompson, T.E., 1994. Semisynthetic proteins: model systems for the study of the insertion of hydrophobic peptides into preformed lipid bilayers. *Biochemistry* 33, 15469–15482.
- Nakajima, N., Ikeda, Y., 1995. Mechanism of amide formation by carbodiimide for bioconjugation in aqueous media. *Bioconjug. Chem.* 6, 123–130.
- Schwendener, R.A., Trub, T., Schott, H., Langhals, H., Barth, R.F., Groscurth, P., Hengartner, H., 1990. Comparative studies of the preparation of immunoliposomes with the use of two bifunctional coupling agents and investigation of in vitro immunoliposome-target cell binding by cytofluorometry and electron microscopy. *Biochim. Biophys. Acta* 1026, 69–79.
- Speth, P.A., van Hoesel, Q.G., Haanen, C., 1988. Clinical pharmacokinetics of doxorubicin. *Clin. Pharmacokinet.* 15, 15–31.
- Takeoka, S., Teramura, Y., Okamura, Y., Handa, M., Ikeda, Y., Tsuchida, E., 2001. Fibrinogen-conjugated albumin polymers and their interaction with platelets under flow conditions. *Biomacromolecules* 2, 1192–1197.
- Takeuchi, H., Kojima, H., Yamamoto, H., Kawashima, Y., 2001. Passive targeting of doxorubicin with polymer coated liposomes in tumor bearing rats. *Biol. Pharm. Bull.* 24, 795–799.
- Woodle, M.C., Lasic, D.D., 1992. Sterically stabilized liposomes. *Biochim. Biophys. Acta* 1113, 171–199.
- Working, P.K., Dayan, A.D., 1996. Pharmacological-toxicological expert report. CAELYX (Stealth liposomal doxorubicin HCl). *Hum. Exp. Toxicol.* 15, 751–785.
- Yamaoka, K., Tanigawara, Y., Nakagawa, T., Uno, T., 1981. A pharmacokinetic analysis program (multi) for microcomputer. *J. Pharmacobiodyn.* 4, 879–885.
- Yuda, T., Maruyama, K., Iwatsuru, M., 1996. Prolongation of liposome circulation time by various derivatives of polyethyleneglycols. *Biol. Pharm. Bull.* 19, 1347–1351.



Pharmaceutical Nanotechnology

Determinants for in vivo anti-tumor effects of PEG liposomal doxorubicin: Importance of vascular permeability within tumors

Ken-ichi Ogawara^a, Keita Un^a, Keiko Minato^a, Ken-ichi Tanaka^b, Kazutaka Higaki^a, Toshikiro Kimura^{a,*}^a Department of Pharmaceutics, Faculty of Pharmaceutical Sciences, Okayama University, 1-1-1 Tsushima-Naka, Okayama 700-8530, Japan^b Department of Clinical Pharmacy, Shujitsu University School of Pharmacy, Okayama 703-8516, Japan

ARTICLE INFO

Article history:

Received 20 November 2007
Received in revised form 25 January 2008
Accepted 15 March 2008
Available online 27 March 2008

Keywords:

Liposome
Doxorubicin
EPR effect
Tumor vasculature
VEGF

ABSTRACT

To elucidate the determinants of the in vivo anti-tumor efficacy of polyethylene glycol (PEG)-modified liposomal doxorubicin (DOX), we examined its anti-tumor effect against three different tumor cell lines (Lewis lung cancer (LLC), Colon-26 (C26) and B16BL6 melanoma (B16)) in vitro and in vivo. In vitro, LLC was the most sensitive tumor to DOX and liposomal DOX based on the MTT assay. However, the strongest in vivo anti-tumor effect was observed in the C26 tumor-bearing mice. The in vivo accumulation of radio-labelled PEG liposome in the C26 tumor after intravenous injection was significantly larger than in other tumors. The extent of vascularity assessed by immunohistochemical staining of CD31 was not directly related with the tumor accumulation of PEG liposome. On the other hand, Evans blue extravasation and secretion of VEGF in C26 tumors were higher than in LLC tumors, clearly demonstrating that the vascular permeability was higher within C26 tumors. These results indicated that the vascular permeability within the tumor substantially affects the tumor accumulation of PEG liposome and may be one of the important determinants in the in vivo anti-tumor efficacy of PEG liposomal DOX.

© 2008 Elsevier B.V. All rights reserved.

1. Introduction

The clinical usefulness of the 3-(4,5-dimethylthiazol-2-yl)-2,5-diphenyl tetrazolium bromide (MTT) assay-based in vitro chemosensitivity test is widely recognized to predict patient responses to particular drugs, allowing for the selection of appropriate chemotherapeutic drugs and the avoidance of ineffective drugs, thereby improving patient survival (Tonn et al., 1994; Nakamura et al., 2006). Accumulating knowledge on this assay revealed its usefulness especially to avoid the administration of ineffective chemotherapeutic drugs to patients. However, there are papers reporting the false-positive results of MTT assay-based selection of drugs (Smit et al., 1992; Kratzke and Kramer, 1996; Shaw et al., 1996). These results indicate that not only the in vitro sensitivity of tumor cells isolated from patients toward a given chemotherapeutic drug but also the in vivo disposition characteristics of the drug including its accessibility to tumor tissue would be the important determinants for the therapeutic outcome in the cancer chemotherapy.

Most solid tumors possess unique pathophysiological characteristics that are not observed in normal tissues/organs, such

as extensive angiogenesis, defective vascular architecture and impaired lymphatic drainage/recovery system. Generally, the capillary permeability of the endothelium in newly vascularized tumors is significantly greater than that of normal organs. Many of drug delivery approaches to target tumors take advantage of these unique pathophysiological properties of tumor vasculatures (Maeda et al., 2000). Due to the long circulation time of polyethylene glycol (PEG)-modified liposomes (PEG liposome) and the leakiness of the microcirculation in the solid tumors, PEG liposome containing anticancer drugs has been shown to accumulate preferentially in the tumors (Unezaki et al., 1996; Gabizon et al., 2006; Heyes et al., 2006). This phenomenon known as the enhanced permeability and retention (EPR) effect has been generally observed in many types of solid tumors and provides a great opportunity for passive targeting of liposomal anticancer agents into the tumor tissue (Northfelt et al., 1998; Schmidt et al., 1998). PEG liposomal doxorubicin (Doxil[®], Caelyx[®]) has been approved for the treatment of several types of cancers in Japan, U.S. and Europe. However, the extent of vascularity and permeability of vasculatures within tumors might be different from one tumor to the other. Therefore, these pathophysiological differences in the tumor may result in the different therapeutic effects in the EPR effect-based therapy. In the present study, we prepared the different tumor-bearing mice models (colon adenocarcinoma, C26; Lewis lung cancer, LLC; and B16BL6 melanoma, B16) and analyzed these pathophysiological

* Corresponding author. Tel.: +81 86 251 7948; fax: +81 86 251 7926.
E-mail address: kimura@pharm.okayama-u.ac.jp (T. Kimura).

characteristics of each tumor. Therapeutic effect of intravenously administered PEG liposomal doxorubicin (DOX) was also evaluated in these tumor-bearing mice models to find out determinants for the EPR effect-based *in vivo* anti-tumor effects of PEG liposomal DOX including the *in vitro* sensitivity of these tumor cells to DOX.

2. Materials and methods

2.1. Materials

Distearoyl phosphatidylethanolamine-*N*-[methoxy poly (ethylene glycol)-2000] (PEG-DSPE) and hydrogenated soybean phosphatidylcholine (HSPC) were purchased from NOF Inc. (Tokyo, Japan). Cholesterol (Chol) and [³H] Cholesteryl hexadecyl ether ([³H] CHE) were purchased from Wako Pure Chemical Industry Inc. (Osaka, Japan) and PerkinElmer Life Science Inc. (Boston, MA, USA), respectively. Doxorubicin (DOX), 3-amino-9-ethylcarbazole (AEC) tablets and 3-(4,5-dimethylthiazol-2-yl)-2,5-diphenyltetrazolium bromide (MTT), Dulbecco's modified Eagle's medium (DMEM), RPMI, fetal bovine serum (FBS) and antibiotics were obtained from Sigma (St. Louis, MO, USA). Rat anti-mouse CD31 or rat anti-mouse vascular endothelial growth factor (VEGF) antibody was purchased from BD Biosciences (San Jose, CA, USA) or from R&D Systems (Minneapolis, MN, USA), respectively. Horse radish peroxidase (HRP)-conjugated rabbit anti-rat IgG or goat anti-rabbit IgG was purchased from Zymed Laboratory (San Francisco, CA). All other chemicals were of the finest grade available.

2.2. Cells

LLC, C26 and B16 were kindly provided from Cell Resource Center for Biomedical Research, Institute of Development, Aging and Cancer, Tohoku University (Sendai, Japan). LLC was cultured in DMEM, and C26 or B16 was cultured in RPMI, both supplemented with 100 U/ml penicillin, 100 µg/ml streptomycin, 20 µg/ml gentamicin and 10% heat-inactivated FBS at 37 °C under 5% CO₂/95% air.

2.3. MTT assay

Sensitivity of each type of tumor cells to DOX was evaluated using 3-(4,5-dimethylthiazol-2-yl)-2,5-diphenyltetrazolium bromide (MTT)-based cytotoxicity assay (Mosmann, 1983). Briefly, cell suspension diluted with the corresponding growth medium was added to each well (3000 cells/well) of a 96-well flat bottom microtitration plate (Asahi Techno Glass, Chiba, Japan). All plates were incubated for 12 h at 37 °C in a humidified 5% CO₂ atmosphere. Nine dilutions (0.01–100 µM) of DOX solution or PEG liposomal DOX were added to each corresponding wells in the plate. After incubation for 48 h, each well was washed and rinsed with growth medium. MTT solution (5 mg/ml) was added to each well and the cultures were further incubated for 4 h at 37 °C. The medium containing MTT was removed from the wells and the remaining MTT-formazan crystals were dissolved by adding 100 µl of 0.04 M HCl-isopropanol. After being subjected to sonication in a bath-type sonicator (ASONE Corporation, Osaka) for 15 min, each plate was set into an ELISA plate reader (Bio-Rad, Hercules, CA) and absorbance at 570 nm (test wavelength) and 750 nm (reference wavelength) were simultaneously measured. The absorbance at reference wavelength was subtracted from the absorbance at test wavelength. Results were expressed as percent cell survival, calculated for each DOX concentration by the following formula:

$$\% \text{ cell survival} = \frac{OD_{570, \text{sample}} - OD_{750, \text{sample}}}{OD_{570, \text{control}} - OD_{750, \text{control}}} \times 100 \quad (1)$$

where sample and control mean the cells with and without DOX treatment, respectively. Percent cell survival was plotted against DOX concentration and was fitted with the Hill-type equation (Eq. (2)) (Eghbali et al., 2003; Lim et al., 2004) using the non-linear least-squares regression program MULTI (Yamaoka et al., 1981). The concentration at which 50% of cells survived corresponded to IC₅₀:

$$E = \frac{E_0 \times IC_{50}}{IC_{50} + C} \quad (2)$$

where E or E_0 is the % cell survival with or without DOX treatment, respectively, and C is the final concentration of DOX in each well. Each experiment was performed using three replicated wells for each DOX concentration and carried out independently five times.

2.4. Liposome preparation

Liposomes were prepared as follows. Lipids from chloroform stock solution of HSPC, Chol, and PEG-DSPE were mixed (HSPC:Chol:PEG-DSPE = 56:38:5 by molar ratio) with trace amount of [³H] CHE, and dried under reduced pressure. For liposomes without DOX, the dried lipid film was hydrated with PBS (pH 7.4) under mechanical agitation. Then, the resulting multilamellar preparations were sized by repeated extrusion through polycarbonate membrane filters (Millipore, Bedford, MA, USA) with the pore size of 200 nm followed by further extrusion through the one with 100 nm. For the preparation of DOX-containing liposome, DOX was encapsulated by remote loading method (Haran et al., 1993). In short, after the dried lipid film was hydrated with 250 mM ammonium sulfate (pH 5.4), the resulting liposomes were passed through a Sephadex G-25 column equilibrated with PBS (pH 8.0) to change the pH of the external phase. DOX in PBS (pH 8.0) was added to liposomes at a drug-to-lipid molar ratio of 1:10 and incubated at 60 °C for 1 h. Our preliminary experiments showed that DOX was efficiently encapsulated into liposomes and the loading efficacy was more than 98% reproducibly. Particle sizes of the liposome were determined by dynamic light scattering spectrophotometer (DLS-7000, Otsuka Electronics, Osaka), and were 94.7 ± 9.4 nm and 96.4 ± 14.8 nm for the empty liposome and DOX-containing liposome, respectively.

2.5. Tumor-bearing mice model

Male BALB/c or C57BL6 mice (6–7 weeks) for the inoculation of C26 or LLC and B16, respectively, were purchased from Charles River Laboratories Inc. (Yokohama, Japan) and maintained at 25 °C and 55% of humidity with free access to standard chow and water. To prepare tumor-bearing mice, 1 million tumor cells were subcutaneously injected in the back of mice. Our investigations were performed after approval by our local ethical committee at Okayama University and in accordance with Principles of Laboratory Animal Care (NIH publication #85-23).

2.6. Tissue distribution

Liposome (10 µmol total lipid/kg) containing trace amount of [³H]-CHE was intravenously administered into tumor-bearing mice when the tumor grew up to 500 mm³ in volume. At 48 h after injection, various organs including the liver, spleen, lung, kidney, heart and tumor were excised for the measurement of radioactivity after washed with saline. To solubilize organs, Soluene-350 (Packard instrument Inc., Meriden, CT, USA) was added and incubated for 2 h at 50 °C before neutralized by HCl. Scintillation medium was added to samples, and radioactivity was determined by a liquid scintillation counter (TRI-CARB® 2260XL, Packard instrument Inc.).

2.7. In vivo anti-tumor activity

When the tumor grew up to 500 mm³ in volume, DOX-containing liposome was administered at a dose of 5 mg/kg DOX by intravenous injection through the tail vein. Saline solution was injected into control group. The tumor volume was measured every other day with a caliper in two dimensions, and was calculated using the following equation: volume (mm³) = longer diameter × (shorter one)² × 0.52 (Lee et al., 2005). The results were expressed as % of initial volume for all tumor models. The experiment was terminated when one of the mice in either control or treatment group died. A slope of % of initial volume–time curve, representing the growth rate of each tumor in the treatment group (T), was obtained (day 11–18, 11–24, or 14–28 for LLC, C26, or B16 tumor, respectively) and divided by that in the control group (C) to give an index (T/C) for the in vivo therapeutic effect for each tumor-bearing mouse model.

2.8. Immunohistochemical staining of CD31 or VEGF within the tumor tissue

Tumor tissues were excised from mice when the tumor grew up to 500 mm³ in volume and snap-frozen in isopentane. Acetone-fixed 5- μ m thick sections of tumor tissues were prepared with the use of cryostat (CM1850, Leica Microsystems, Wetzlar, Germany). Then, the tumor sections were incubated with rat anti-mouse CD31 antibody or VEGF antibody diluted in PBS containing 5% FBS. This was followed by incubation with horse radish peroxidase (HRP)-conjugated rabbit anti-rat IgG antibody and further incubation with HRP-conjugated goat anti-rabbit IgG antibody. Peroxidase visualization was performed by the conventional staining procedure with 3-amino-9-ethyl-carbazole (AEC, Sigma), and the sections were counterstained with Mayers hematoxylin (Merck, Darmstadt, Germany) according to standard laboratory protocols. In the case of CD31 staining, the staining procedure was followed by the counting of the number of vessels under the microscope in ten independent fields for each type of tumor cells.

2.9. Extravasation of albumin-Evans blue within tumor tissues

Evans blue dissolved in saline (1 mg/mL) was administered into the tail vein of tumor-bearing mice at a dose of 4 mg/kg. Forty-eight hours after intravenous injection, tumors were excised and were snap-frozen. Cross-sections of tumor tissues were prepared as described above and were directly subjected to the observation under the microscope equipped with digital recording system (VH-5000, KEYENCE, Osaka).

2.10. Enzyme-linked immunosorbent assay for VEGF

Tumor tissues with 500 mm³ in volume were homogenized in lysis buffer containing 5% protease inhibitor cocktail (Sigma). VEGF levels were quantified with commercially available enzyme-linked immunosorbent assays (Mouse VEGF ELISA kit, BioSource International, Inc., Camerillo, CA).

2.11. Statistical analysis

Results are expressed as the mean \pm S.D. Analysis of variance (ANOVA) was used to test the statistical significance of differences among groups. Statistical significance was evaluated by using Student's *t*-test or Dunnett's test for the single or multiple comparisons of experimental groups, respectively.

3. Results and discussion

To have an optimal in vivo anti-tumor effect in the cancer chemotherapy, many factors that influence the therapeutic outcome should be taken into consideration. Among them, the sensitivity of tumor cells composing a tumor tissue against the anticancer drug used is one of the most important factors. Irrespective of the approaches to improve the drug delivery into tumor tissues, the tumor cells with very low sensitivity to a given anticancer drug will not be efficiently killed with the drug. On the other hand, it was reported that anticancer drugs with high sensitivity did not always lead to the good therapeutic outcome (Smit et al., 1992; Kratzke and Kramer, 1996; Shaw et al., 1996).

In the present study, to elucidate the important determinants for the EPR effect-based in vivo anti-tumor effect of PEG liposomal DOX, we first evaluated the sensitivity of each type of tumor cells tested to DOX solution (Fig. 1a). The obtained results revealed that LLC had the smallest IC₅₀ value (0.096 μ M) among the three tumor cells studied, indicating that LLC was the most sensitive to DOX solution. B16 tended to show the larger IC₅₀ value (0.213 μ M) than LLC, and C26 showed significantly larger IC₅₀ value (0.311 μ M) than LLC, suggesting the lower sensitivity to DOX. We also performed the similar study using PEG liposomal DOX (Fig. 1b). It was confirmed that the order of sensitivity of the three tumor cells was the same as that for DOX solution and C26 showed significantly larger IC₅₀ value

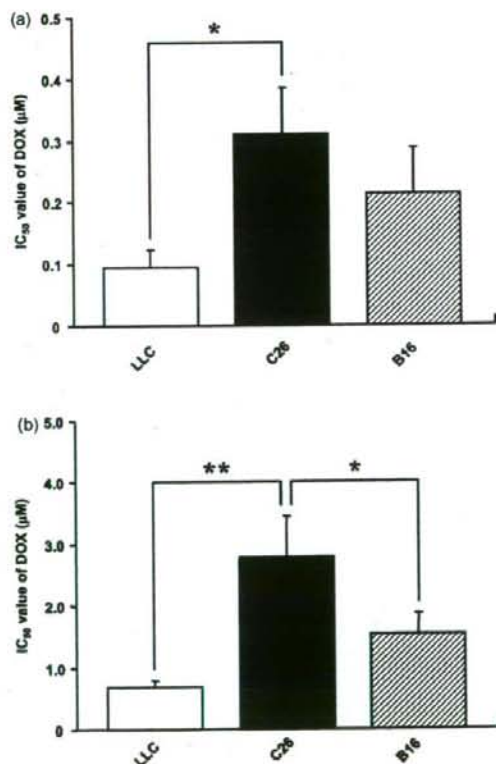


Fig. 1. In vitro sensitivity of Lewis lung cancer (LLC), Colon-26 (C26) and B16BL6 melanoma (B16) cells to DOX solution (a) and PEG liposomal DOX (b). Results are expressed as the mean with the vertical bar showing S.D. of five independent experiments. ***p* < 0.01, **p* < 0.05.

Table 1
Tumor growth rates and T/C values in tumor-bearing mice

	Tumor growth rate (% of initial/day)		T/C
	Control (saline)	PEG liposomal DOX	
LLC	205 ± 72	51.8 ± 18.0 [*]	0.35 ± 0.09 [*]
C26	37.6 ± 8.9	2.71 ± 7.47 ^{***}	0.07 ± 0.20
B16	123 ± 37	57.2 ± 33.2 [*]	0.46 ± 0.27 [*]

Tumor growth rate was estimated as the slope of tumor growth-time curve calculated based on day 11–18, 11–24, or 14–28 for LLC, C26, or B16 tumor, respectively. T/C values were calculated as the ratio of PEG liposomal DOX treated- to control groups in tumor growth rate.

^{*} $p < 0.05$.

^{***} $p < 0.001$, compared with each control group.

^{*} $p < 0.05$, compared with C26.

than other tumor cells, suggesting the lowest sensitivity to DOX. The absolute IC_{50} values for PEG liposomal DOX (LLC, 0.68 μ M; C26, 2.5 μ M; B16, 1.4 μ M) were about 10 times larger than DOX solution, reflecting the slow release rate of doxorubicin from PEG liposome.

In vivo anti-tumor effect of PEG liposomal DOX was also studied in the mice bearing C26, LLC or B16 tumor (Fig. 2 and Table 1). Significant in vivo anti-tumor effects of liposomal DOX were observed in all the tumor models studied. On the day when we terminated the experiment, the size of C26 tumor treated with liposomal DOX was much smaller (around 200% of the initial volume) than other tumors investigated (Fig. 2). Since the tumor growth rate was different depending on the type of tumors, we also calculated the index for the in vivo therapeutic effect (T/C) that is independent of the growth rate of each type of tumors, to compare the in vivo efficacy of liposomal DOX and were summarized in Table 1. Calculation of T/C also gave the significantly lower value (0.07 ± 0.20) for C26 tumor-bearing mice than other two tumors (LLC, 0.35 ± 0.09; B16, 0.46 ± 0.27). From these results, it was revealed that the strongest in vivo anti-tumor effect was observed in the C26 tumor model, and that the in vivo anti-tumor effect of PEG liposomal DOX was not directly reflecting the sensitivity of tumor cells against DOX.

The in vivo disposition characteristics of intravenously administered PEG liposome must be taken into considerations as one of the crucial factors for the therapeutic outcome of PEG liposomal DOX. It was reported that DOX injected as a solution was so rapidly eliminated from plasma by being excreted into bile and urine and that

the amount of DOX distributed into tumor tissues was very small (Gabizon et al., 1996; Mayer et al., 1989). PEG liposomal preparation can improve the retention of DOX in plasma, but to exert the in vivo anti-tumor effect of PEG liposomal DOX, certain amount of DOX-containing PEG liposome must be extravasated to get into the tumor tissue, and DOX must be released and taken up by the surrounding tumor cells. In plasma, DOX leakage from the liposome with the same lipid composition as those applied in this study was very slow ($T_{1/2} = 100$ h) and the presence of fluid obtained from malignant effusions significantly elevated the release rate (Gabizon, 1995). Therefore, DOX would be mainly released from PEG liposome after the liposome is extravasated within the tumor tissue. Considering the low leakage of DOX from PEG liposome in the blood circulation, the in vivo disposition characteristics of PEG liposomal DOX would be similar to the one of PEG liposome. Therefore, we evaluated the in vivo distribution characteristics of ³H-labeled PEG liposome by measuring radioactivity.

Tissue distribution of PEG liposome at 48 h after intravenous administration was investigated in the mice bearing C26, LLC or B16 tumor of 500 mm³ in volume (Fig. 3). Tissue distribution of PEG liposome exhibited the similar tendency for each tumor-bearing mice, and it was found that PEG liposome mainly distributed to the liver and spleen irrespective of the type of tumors. On the other hand, the distribution of PEG liposome into tumor was quite different depending on the type of the tumors used, and the disposition amount of PEG liposome in the C26 tumor was significantly and approximately threefold larger than those in the other two tumors. These results suggest that the tumor accumulation of PEG liposome correlates with the in vivo anti-tumor efficacy of PEG liposomal doxorubicin in these tumors.

After its systemic administration, the liposome follows two distinct processes before its accumulation into tumors, i.e., circulation within vessels (blood circulation) and transport across vasculature walls into the surrounding tumor tissues (extravasation). Generally, extravasation of particles in blood circulation is a function of both local blood flow and vascular permeability. One of the factors that influence the local blood flow is the extent of vascularity within the tissue. That is to say, the tissue with numerous vasculatures will receive larger local blood supply. To unravel the mechanism underlying the larger tumor accumulation of PEG liposome in C26 tumor, we evaluated the extent of vascularity in each type of tumor tis-

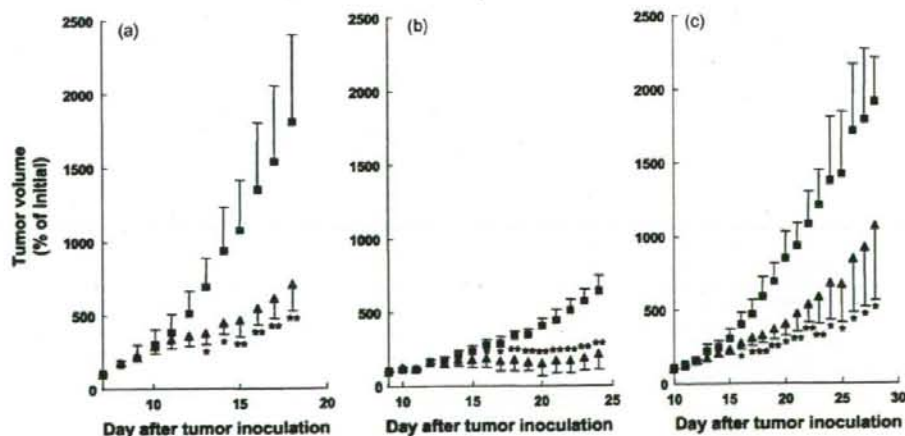


Fig. 2. In vivo anti-tumor effect of PEG liposomal DOX in tumor-bearing mice. Tumor volume was expressed as % of initial volume (around 500 mm³) for all tumor models. Results are expressed as the mean with the bar showing S.D. of five experiments. ^{*} $p < 0.05$; ^{**} $p < 0.01$, compared with saline treatment. (a) LLC-bearing mice; (b) C26-bearing mice; (c) B16-bearing mice. Keys: (■) saline treatment; (▲) PEG liposomal DOX treatment. DOX dose was 5.0 mg/kg.

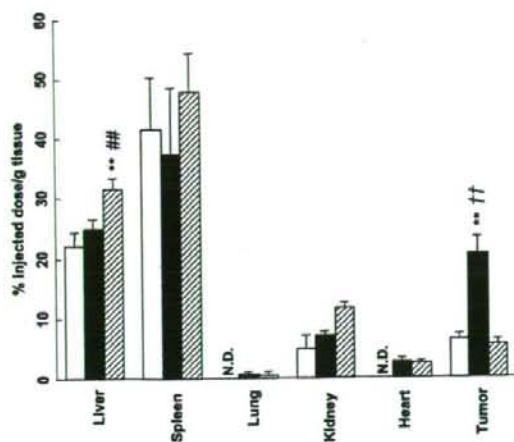


Fig. 3. Tissue distribution of PEG liposomes at 48 h after intravenous administration into tumor-bearing mice. Keys: (□) LLC-bearing mice; (■) C26-bearing mice; (▨) B16-bearing mice. Results are expressed as the mean with the bar showing S.D. of three experiments. ** $p < 0.01$, compared with LLC-bearing mice; ## $p < 0.01$, compared with C26-bearing mice; †† $p < 0.01$, compared with B16-bearing mice. Dose of liposome was $10 \mu\text{mol}$ total lipid/kg.

sue. To visualize the vasculature, cryostat sections were incubated with rat antibody recognizing the mouse endothelial cell marker CD31, followed by the standard staining procedure as described in Section 2. As shown in Fig. 4, in the sections prepared from LLC and B16 tumors, tube-like large vessels were often observed but the numbers of vessels were relatively small (LLC, 28 ± 5 ; B16, 17 ± 6 vessels per field). On the other hand, a lot of tiny vessels (47 ± 6 vessels per field) equally distributed throughout the tumor tissue were observed in C26 tumor.

Besides the extent of vascularity, the permeability of vasculature within the tumor tissue would be one of the important factors influencing the transport of liposome across vasculature walls (Yuan et al., 1995) and may vary considerably depending on the type of tumor models. Several earlier studies demonstrated the differences in the vascular permeability of macromolecules among the tumor tissues used (Graff et al., 2000, 2001; Dreher et al., 2006). Evans blue was utilized to evaluate the vascular permeability of tumor tissues, because the dye spontaneously makes a complex with serum albumin by electrostatic interaction between the sulfonic acid group of the dye and the terminal cationic nitrogens of the lysine residues of albumin (Clasen et al., 1970) and it has, therefore, been generally applied to evaluate the vascular permeability within tumor tissues (Amice et al., 1978; Roberts and Hasan, 1993; Tanaka et al., 2003). Since it was previously reported that the amount of Evans blue

remaining in the blood is negligible at 48 h after its intravenous administration at 10 mg/kg (Graff et al., 2000), we excised tumor tissues at 48 h after intravenous administration in order to discriminate Evans blue extravasated from that in blood vessels. In C26 tumor, the blue color derived from Evans blue was able to be clearly observed equally throughout the tumor (Fig. 5b), suggesting that the permeability of vasculature within C26 tumor would be high and the equal distribution of tiny vasculature throughout the tumor would also be responsible for this observation. On the other hand, in the case of LLC tumor, the blue color was hardly found (Fig. 5a), indicating that the permeability of vasculatures in LLC tumor is very low and that the vascularity is not necessarily a sufficient factor for the efficient intra-tumoral accumulation of PEG liposome. Unfortunately, we were not able to perform the similar study for B16 tumor due to the intrinsic black color of the tissue. Although we did not see any direct relationship between the extent of vascularity (Fig. 4) and the tumor accumulation characteristics of PEG liposome (Fig. 3), the results on Evans blue extravasation obtained for C26 and LLC tumors (Fig. 5) could explain the difference in the tumor accumulation of PEG liposome between the two tumor tissues. That is to say, not only the extent of vascularity within the tumor but also the vascular permeability would be responsible for the accumulation of PEG liposome into tumor tissues. Therefore, the vascular permeability within the tumor would be one of the crucial determinants in the *in vivo* anti-tumor effect of PEG liposomal DOX. To draw more universal conclusion on this issue, however, increasing the number of tumor types investigated would be necessary and will be the subject of our further study. In addition, intra-tumoral distribution pattern of PEG liposome would also be an important factor to determine the *in vivo* anti-tumor effect. Although we did not directly evaluate the intra-tumoral distribution of PEG liposome, we consider that the intra-tumoral distribution of extravasated Evans blue would be reflecting that of PEG liposome. Therefore, it can be considered that the higher permeability of vasculature and the equal distribution of tiny vasculature observed in the case of C26 tumor would be beneficial for the efficient intra-tumoral distribution of PEG liposome. Together with these factors, the difference in the extent of vascularity between central and peripheral parts of tumor tissue and/or the interstitial fluid pressure may vary depending on the type of tumor and would affect the intra-tumoral distribution of PEG liposome.

One of the major factors that influence the vascular permeability within the tumor tissue is VEGF (Kliche and Waltenberger, 2001). To unravel the mechanism underlying the difference in vascular permeability between C26 and LLC tumors, we performed immunohistochemical staining of VEGF within the tumor tissues for the semi-quantification (Fig. 6a and b). As shown in Fig. 6a and b, the higher amount of VEGF in C26 tumor than LLC tumor was detected. Furthermore, the quantification of VEGF amount in each tumor by ELISA demonstrated that approximately eightfold larger

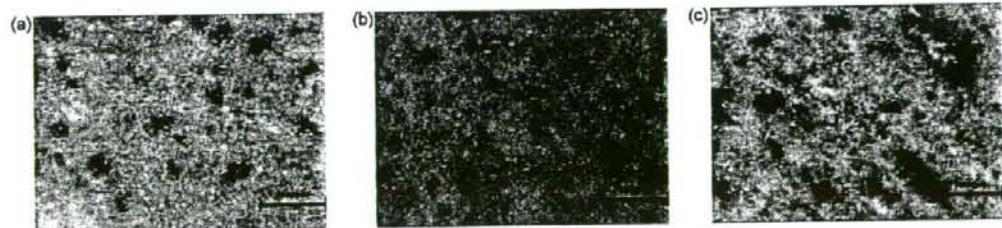


Fig. 4. Immunohistochemical staining of CD31 in each tumor section of LLC (a), C26 (b), and B16 tumors (c). Tumor tissues were excised from mice when the tumor became 500 mm^3 in volume and were snap-frozen. Acetone-fixed $5\text{-}\mu\text{m}$ thick sections of tumor tissues were prepared and then AEC staining was performed for CD31 as described in Section 2. Bar: $100 \mu\text{m}$.

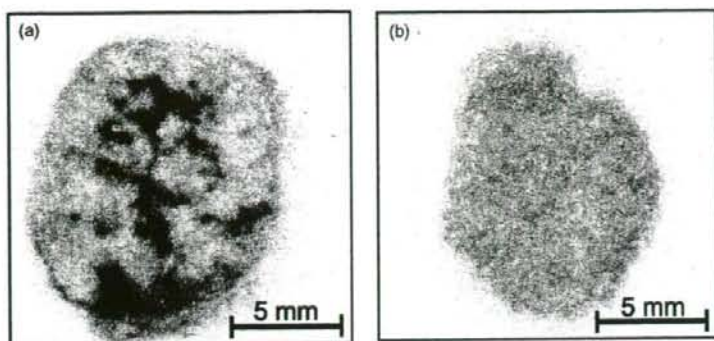


Fig. 5. Extravasation of Evans blue in LLC (a) and C26 tumors (b). Forty-eight hours after intravenous injection of Evans blue solution, tumors were excised and were snap-frozen. Cross-sections of tumor tissues were directly subjected to the observation under the microscope as described in Section 2. The result shown here is the representative one among three independent tumor sections per group.

amount of VEGF was secreted in C26 tumor compared with that of LLC tumor (Fig. 6c). From these results, it was suggested that the higher vascular permeability within C26 tumor (Fig. 5) would be ascribed to its higher secretion of VEGF within the tumor tissue.

Mediators that would be substantially responsible for enhancing the secretion of VEGF in these tumor tissues remain unclear, but should be identified for the development of the more efficient cancer chemotherapy.

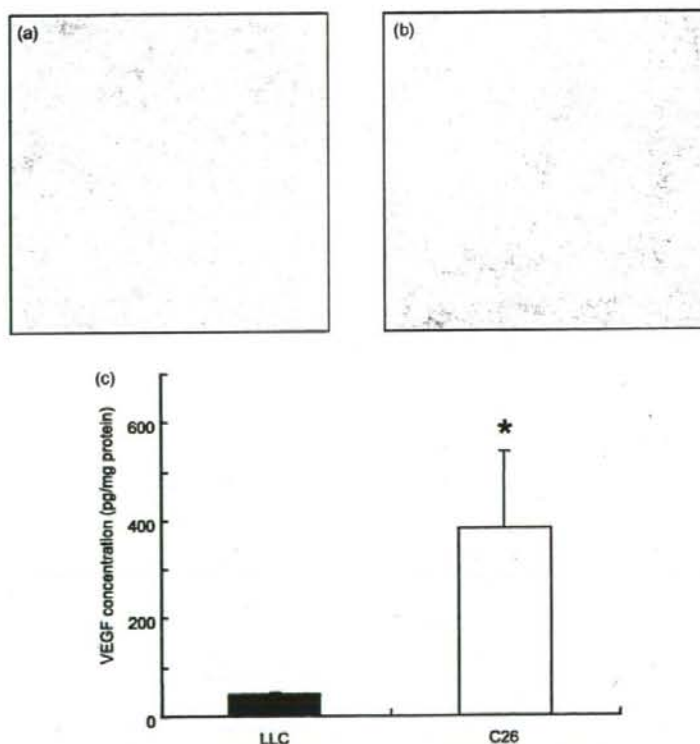


Fig. 6. Immunohistochemical staining of VEGF in LLC (a) and C26 tumors (b), and quantification of VEGF amount within the tumor tissue by ELISA (c). Tumor tissues were excised from mice when the tumor became 500 mm³ in volume and were snap-frozen. Acetone-fixed 5- μ m thick sections of tumor tissues were prepared and then AEC staining was performed for VEGF as described in Section 2. In parallel, tumor tissues were homogenized in lysis buffer containing 5% protease inhibitor cocktail and VEGF levels were quantified with commercially available ELISA kit. Results are expressed as the mean with the vertical bar showing S.D. of four independent experiments. * $p < 0.05$, compared with LLC.

The present study clearly demonstrated that besides the improvement of retention of liposomal DOX in plasma, the higher vascular permeability within tumor tissues would also be required for liposomal DOX to be taken up more efficiently by tumor cells, indicating that the permeability of vasculature within tumor tissues is a critical factor for EPR effect-based anti-tumor effect of liposomal DOX.

References

- Amice, J., Dazord, L., Toujas, L., 1978. Impairment of inflammatory reactions in tumour-bearing mice as measured by Evans blue extravasation. *Eur. J. Cancer* 14, 1287–1289.
- Clasen, R.A., Pandolfi, S., Hass, G.M., 1970. Vital staining, serum albumin and the blood-brain barrier. *J. Neuropathol. Exp. Neurol.* 29, 266–284.
- Dreher, M.R., Liu, W., Michelich, C.R., Dewhirst, M.W., Yuan, F., Chilkoti, A., 2006. Tumor vascular permeability, accumulation, and penetration of macromolecular drug carriers. *J. Natl. Cancer Inst.* 98, 335–344.
- Eghbali, M., Birnir, B., Gage, P.W., 2003. Conductance of GABA_A channels activated by pentobarbitone in hippocampal neurons from newborn rats. *J. Physiol.* 552, 13–22.
- Gabizon, A.A., 1995. Liposome circulation time and tumor targeting: Implications for cancer chemotherapy. *Adv. Drug Del.* 16, 285–294.
- Gabizon, A.A., Chemla, M., Tzemach, D., Horowitz, A.T., Goren, D., 1996. Liposome longevity and stability in circulation: effects on the in vivo delivery to tumors and therapeutic efficacy of encapsulated anthracyclines. *J. Drug Target.* 3, 391–398.
- Gabizon, A.A., Shmeeda, H., Zalipsky, S., 2006. Pros and cons of the liposome platform in cancer drug targeting. *J. Liposome Res.* 16, 175–183.
- Graff, B.A., Bjornaes, I., Rofstad, E.K., 2000. Macromolecule uptake in human melanoma xenografts: relationships to blood supply, vascular density, microvessel permeability and extracellular volume fraction. *Eur. J. Cancer* 36, 1433–1440.
- Graff, B.A., Bjornaes, I., Rofstad, E.K., 2001. Microvascular permeability of human melanoma xenografts to macromolecules: relationships to tumor volumetric growth rate, tumor angiogenesis and VEGF expression. *Microvascul. Res.* 61, 187–198.
- Haran, G., Cohen, R., Bar, L.K., Barenholz, Y., 1993. Transmembrane ammonium sulfate gradient in liposomes produce efficient and stable entrapment of amphipathic weak bases. *Biochim. Biophys. Acta* 1151, 201–215.
- Heyes, J., Hall, K., Tailor, V., Lenz, R., MacLachlan, L., 2006. Synthesis and characterization of novel poly(ethylene glycol)-lipid conjugates suitable for use in drug delivery. *J. Control. Release* 112, 280–290.
- Kliche, S., Waltenerberger, J., 2001. VEGF receptor signaling and endothelial function. *IUBMB Life* 52, 61–66.
- Kratzke, R.A., Kramer, B.S., 1996. Evaluation of in vitro chemosensitivity using human lung cancer cell lines. *J. Cell Biochem.* 24, 160–164.
- Lee, E.S., Na, K., Bae, Y.H., 2005. Doxorubicin loaded pH-sensitive polymeric micelles for reversal of resistant MCF-7 tumor. *J. Control. Release* 103, 405–418.
- Lim, J.G., Lee, H.Y., Yun, J.E., Kim, S.P., Park, J.W., Kim, S.S., Han, J., Park, M.J., Song, D.K., 2004. Taurine block of cloned ATP-sensitive K⁺ channels with different sulfonylurea receptor subunits expressed in *Xenopus laevis* oocytes. *Biochem. Pharmacol.* 68, 901–910.
- Maeda, H., Wu, J., Sawa, T., Matsumura, Y., Hori, K., 2000. Tumor vascular permeability and the EPR effect in macromolecular therapeutics: a review. *J. Control. Release* 65, 271–284.
- Mayer, L.D., Tai, L.C., Ko, D.S., Masin, D., Ginsberg, R.S., Cullis, P.R., Bally, M.B., 1989. Influence of vesicle size, lipid composition, and drug-to-lipid ratio on the biological activity of liposomal doxorubicin in mice. *Cancer Res.* 49, 5922–5930.
- Mosmann, T., 1983. Rapid colorimetric assay for cellular growth and survival: application to proliferation and cytotoxicity assays. *J. Immunol. Methods* 65, 55–63.
- Nakamura, R., Saikawa, Y., Kubota, T., Kumagai, A., Kiyota, T., Ohashi, M., Yoshida, M., Otani, Y., Kumai, K., Kitajima, M., 2006. Role of the MTT chemosensitivity test in the prognosis of gastric cancer patients after postoperative adjuvant chemotherapy. *Anticancer Res.* 26, 1433–1437.
- Northfelt, D.W., Dezube, B.J., Thommes, J.A., Miller, B.J., Fischl, M.A., Friedman-Kien, A., Kaplan, L.D., Mond, C.D., Mamelok, R.D., Henry, D.H., 1998. Pegylated-liposomal doxorubicin versus doxorubicin, bleomycin, and vincristine in the treatment of AIDS-related Kaposi's sarcoma: results of a randomized phase III clinical trial. *J. Clin. Oncol.* 16, 2445–2451.
- Roberts, W.G., Hasan, T., 1993. Tumor-secreted vascular permeability factor/vascular endothelial growth factor influences photosensitizer uptake. *Cancer Res.* 53, 153–157.
- Schmidt, P.G., Adler-Moore, J.P., Forssen, E.A., Proffitt, R.T., 1998. Unilamellar liposomes for anticancer and antifungal therapy. In: Lasic, D.D., Papahadjopoulos, D. (Eds.), *Medical Applications of Liposomes*. Elsevier Science BV, New York, pp. 703–731.
- Shaw, G.L., Gazdar, A.F., Phelps, R., Steinberg, S.M., Linnoila, R.I., Johnson, B.E., Oie, H.K., Russell, E.K., Ghosh, B.C., Pass, H.I., Minna, J.D., Mulshine, J.L., Ihde, D.C., 1996. Correlation of in vitro drug sensitivity testing results with response to chemotherapy and survival: comparison of non-small cell lung cancer and small cell lung cancer. *J. Cell Biochem.* 24, 173–185.
- Smit, E.F., de Vries, E.G., Timmer-Bosscha, H., de Leij, L.F., Oosterhuis, J.W., Scheper, R.J., Weening, J.J., Postmus, P.E., Mulder, N.H., 1992. In vitro response of human small-cell lung-cancer cell lines to chemotherapeutic drugs: no correlation with clinical data. *Int. J. Cancer* 51, 72–78.
- Tanaka, S., Akaike, T., Wu, J., Fang, J., Sawa, T., Ogawa, M., Beppu, T., Maeda, H., 2003. Modulation of tumor-selective vascular blood flow and extravasation by the stable prostaglandin 12 analogue beraprost sodium. *J. Drug Target.* 11, 45–52.
- Tonn, J.C., Schachenmayr, W., Kraemer, H.P., 1994. In vitro chemosensitivity test of malignant gliomas: clinical relevance of test results independent of adjuvant chemotherapy. *Anticancer Res.* 14, 1371–1375.
- Unezaki, S., Maruyama, K., Hosoda, J.I., Nagae, I., Koyanagi, Y., Nakata, M., Ishida, O., Iwatsuru, M., Tsuchiya, S., 1996. Direct measurement of the extravasation of polyethyleneglycol-coated liposomes into solid tumor tissue by in vivo fluorescence microscopy. *Int. J. Pharm.* 144, 11–17.
- Yamaoka, K., Tanigawa, Y., Nakagawa, T., Uno, T., 1981. A pharmacokinetic analysis program (MULTI) for microcomputer. *J. Pharmacobiodyn.* 4, 879–885.
- Yuan, F., Dellian, M., Fukumura, D., Leunig, M., Berk, D.A., Torchilin, V.P., Jain, R.K., 1995. Vascular permeability in a human tumor xenograft: molecular size dependence and cutoff size. *Cancer Res.* 55, 3752–3756.



ELSEVIER

International Journal of Pharmaceutics

journal homepage: www.elsevier.com/locate/ijpharm

Pharmaceutical Nanotechnology

Prolongation of residence time of liposome by surface-modification with mixture of hydrophilic polymers

Tamer Shehata, Ken-ichi Ogawara, Kazutaka Higaki, Toshikiro Kimura*

Department of Pharmaceutics, Faculty of Pharmaceutical Sciences, Okayama University, 1-1-1 Tsushima-naka, Okayama 700-8530, Japan

ARTICLE INFO

Article history:

Received 7 January 2008

Received in revised form 14 March 2008

Accepted 6 April 2008

Available online 12 April 2008

Keywords:

PEG liposome

Polyvinyl alcohol

Pharmacokinetics

Opsonins

Dysopsonins

ABSTRACT

The objective of this study is to evaluate the biodistribution characteristics of liposomes surface-modified with the mixture of polyethylene glycol (PEG) and polyvinyl alcohol (PVA) as a drug carrier for passive targeting of drugs. The liposomes (egg phosphatidylcholine:cholesterol = 55:40, molar ratio) modified with both PEG and PVA (4:1 molar ratio) (PEG4%/PVA1% liposome) provided the largest AUC, which could be attributed to the smallest hepatic clearance of the liposomes. The liver perfusion studies clearly indicated that lower hepatic disposition of PEG4%/PVA1% liposome was ascribed to the decrease in its hepatic uptake via receptor-mediated endocytosis. Furthermore, the amounts of whole serum proteins and of opsonins such as complement C3 and immunoglobulin G adsorbed on PEG4%/PVA1% liposome were significantly smaller than those on the liposome solely modified with PEG (PEG5% liposome). On the other hand, several proteins were adsorbed at larger amount on PEG4%/PVA1% liposome than PEG5% liposome, and the protein identification by LC-MS/MS suggested that some of those proteins including albumin might function as dysopsonins. The decrease in the adsorbed amount of several opsonins and the increase in the adsorbed dysopsonins would be responsible for its lower affinity to the liver and long residence in the systemic circulation of PEG4%/PVA1% liposome.

© 2008 Elsevier B.V. All rights reserved.

1. Introduction

Liposomes, mainly made from naturally occurring phospholipids, are biocompatible vehicles. Liposomes can entrap both hydrophilic and hydrophobic drugs in their aqueous internal compartment or within their membrane bilayer, respectively, and hence it can protect the entrapped drug from external destructive condition such as light, pH and enzymes. Therefore, liposomes are considered to be one of the advantageous candidates of drug carriers (Lian and Ho, 2001; Torchilin, 2005). In spite of these merits, their rapid clearance by the reticuloendothelial system (RES) limits their application as drug carriers to other tissues and/or cells (Poste et al., 1982; Senior, 1987; Allen et al., 1991). Various strategies have been developed in order to avoid RES uptake, including the modifying of the liposomal surface with natural polysaccharides such as mannan, pullulan, amylopectin and dextran (Sihorkar and Vyas, 2001). Besides these approaches, long circulating liposomes were developed by the incorporation of ganglioside GM1, phosphatidylinositol or lipid-conjugated polyethylene glycol (PEG) onto the surface (Allen and Chonn, 1987; Gabizon and Papahadjopoulos, 1988; Allen and Hansen, 1991). Among them, many studies have

demonstrated that PEG-modified liposome exhibits its prolonged blood circulating property by inhibiting adsorption of various opsonins such as immunoglobulin G (IgG) and complement-related components (Banerjee, 2001; Ishida et al., 2002). PEG liposome has been widely used in an attempt to achieve a passive targeting of drugs due to its easy preparation, relatively low cost and its multiple linkability to other lipids (Allen et al., 1991; Maruyama et al., 1999). Lately, the feasibility of modifying the surface of liposomes with polyvinyl alcohol (PVA) or polyacrylic acid (PAA) having a hydrophobic anchor(s) was reported, and it was confirmed that the modification of the liposomal surface with PVA could improve the physical stability of liposomes (Takeuchi et al., 1998, 2000). In addition, the blood circulation time of PVA (MW: 20,000)-modified liposome was comparable to that of PEG (MW: 2000)-liposome (Takeuchi et al., 2001). However, there has been no report examining the effect of the modification of liposomes with the mixture of different hydrophilic polymers. In order to develop the longer circulating liposomal preparations, therefore, we formulated the liposomes surface-modified with the mixture of PEG and PVA, and evaluated their biodistribution characteristics in rats. The hepatic disposition characteristics of these liposomes were evaluated in the liver perfusion experiments. In addition, to have a better understanding of their *in vivo* behavior, especially their hepatic uptake, the interaction of these polymer-modified liposomes with blood components was also studied.

* Corresponding author. Tel.: +81 86 251 7948; fax: +81 86 251 7926.
E-mail address: kimura@pharm.okayama-u.ac.jp (T. Kimura).

2. Materials and methods

2.1. Materials

Egg yolk phosphatidylcholine (EPC), cholesterol (Chol) and distearoyl phosphatidylethanolamine-*N*-[methoxy poly(ethylene glycol)-2000] (PEG-DSPE) were purchased from ASAHI KASEI Chemicals Industry Inc. (Tokyo, Japan), Wako Pure Chemical Industry Inc. (Osaka, Japan) and NOF Inc. (Tokyo), respectively. [³H] Cholesteryl hexadecyl ether ([³H] CHE) was purchased from PerkinElmer Life Science Inc. (Boston, MA, USA). Polyvinyl alcohol derivatives bearing a hydrophobic anchor (C₁₂H₂₅-S-) at the terminal of the molecule with molecular weight of 20,000 was a kind gift from Kuraray Co. (Tokyo). Trypsin from porcine pancreas was purchased from Sigma (St. Louis, MO, USA). Calcein was purchased from Kanto Chemical Co. Inc. (Tokyo). Phospholipid content of liposomes was determined using Phospholipid C-Test Wako (Wako Pure Chemical, Osaka). Rabbit anti-rat IgG polyclonal antibody or goat anti-rat complement C3 polyclonal antibody was purchased from Southern Biotech. (Birmingham, AL, USA) or from MP Biomedicals, LLC (Solon, OH, USA), respectively. All other reagents were of the finest grade available.

2.2. Preparation of liposomes

Small unilamellar liposomes were prepared by the hydration method reported previously (Furumoto et al., 2007). PEG2000 is almost completely incorporated into liposomes at 5 mol% of total lipid contents, but its amount incorporated is saturated over 5–7 mol% (Allen et al., 1991). Therefore, we set the total polymer content to be 5 mol%. EPC, Chol and/or PEG-DSPE from stock solution were mixed at the molar ratio of EPC:Chol = 60:40 for conventional liposome or EPC:Chol:polymer(s) = 55:40:5 for polymer-modified liposomes, respectively, the liposomes were radiolabeled by incorporating trace amount of the non-exchangeable, non-metabolizable marker [³H] CHE to follow the biodistribution of liposomes (Stein et al., 1980). Then, the lipid mixture was dried under reduced pressure. The resultant dried lipid film was hydrated with phosphate-buffered saline (PBS, pH 7.4) under mechanical agitation. The obtained liposomal suspensions were extruded through polycarbonate membrane filters (Millipore, Temecula, CA, USA) with pore sizes of 200 nm 5 times, followed by the extrusion through 100-nm filter 10 times. In order to prepare liposomes-containing PVA, furthermore, an aliquot of the liposomal suspensions were mixed with PVA polymer solution with various concentrations to give an intended final PVA content and was followed by the incubation at 10 °C for 60 min according to the method reported previously (Takeuchi et al., 1998). In the case of calcein-containing liposomes, the hydration of dried lipid film was performed with PBS (pH 7.4) containing calcein (0.2 mg/mL), then the liposomal suspensions were obtained by following the same procedure as described above. Non-encapsulated calcein was removed by gel-filtration chromatography (Sepharose CL-4B, Amersham Bioscience, Uppsala, Sweden). The amount of PVA associated onto the liposomes was estimated by the method reported previously (Takeuchi et al., 1998). In brief, 0.3 mL of liposomal suspension was ultra-centrifuged at 300,000 × g for 120 min. The mixture of 3 mL of boric acid solution (4%, w/v) and 0.6 mL of I₂/KI solution (0.05 M/0.15 M) was added to 0.05 mL of the supernatant, then the solution was diluted to 10 mL with distilled water. The polymer concentration was measured spectrophotometrically at the wavelength of 620 nm. The amount of associated PVA was calculated by subtracting the PVA amount in the solution. It was confirmed that more than 90% of added PVA was incorporated into the liposomal membranes.

2.3. Liposomal size distribution and zeta potential measurements

The size distribution and zeta potentials of liposomes in PBS (pH 7.4) were determined by dynamic light scattering spectrophotometer (DLS-7000, Otsuka Electronics, Osaka) and by electrophoretic light scattering spectrophotometer (ELS-6000, Otsuka Electronic), respectively.

2.4. In vitro release of calcein from liposome

The in vitro release of calcein from liposomes was evaluated by equilibrium dialysis method. In brief, 1 mL of liposomal suspension was mixed with 1 mL of PBS (pH 7.4) containing 10% serum (v/v) and the mixture was loaded into the membrane tube (Spectra/Por[®] Membrane, MWCO: 12,000–14,000, Spectrum Laboratories Inc., Breda, The Netherlands). After both ends were tightly closed, the dialysis tubes were placed into 40 mL of PBS (pH 7.4) as an acceptor medium, and were incubated at 37 °C for 12 h. The percentage of released calcein from liposomes was calculated as follows:

$$\text{release (\%)} = \frac{I_r - I_0}{I_{\text{total}} - I_0} \times 100$$

where I_0 and I_r are the fluorescence intensities of calcein before and after incubation, respectively. I_{total} was the fluorescence intensity of total calcein loaded into liposomes, which was determined after the destabilization of liposomes by 5% Triton X-100 (final concentration). The fluorescence intensity of calcein was measured at 490 and 520 nm for excitation and emission wavelengths, respectively.

2.5. Animals

Male Wistar rats (Japan SLC, Hamamatsu, Japan), maintained at 25 °C and 55% humidity, were allowed free access to standard laboratory chow (Clear Japan, Tokyo) and water. Rats weighing 220–240 g were randomly assigned to each experimental group. Our investigations were performed after approval by our local ethical committee at Okayama University and in accordance with Principles of Laboratory Animal Care (NIH publication #85-23).

2.6. In vivo disposition experiments

After rats were anesthetized by intraperitoneal injection of sodium pentobarbital (20 mg/kg), liposomes were injected into the femoral vein at a dose of 10 μmol total lipid/kg. Body temperature of rats was kept at 37 °C using a heat lamp during the experiment. Blood samples were withdrawn from the jugular vein at fixed time points, followed by immediate centrifugation at 4000 × g. The obtained plasma was collected (100 μL) and scintillation medium (Clear-sol II, Nacal Tesque, Kyoto) was added. For the tissue distribution study, organs (liver, spleen, kidney, heart and lung) were excised at 6 h after the intravenous injection, rinsed with PBS, and weighed. To solubilize the organs, Soluene-350 (Packard Instrument Inc., Meriden, CT, USA) was added and incubated for 2 h at 50 °C before the solubilized solution was neutralized by HCl. Then, scintillation medium was added to the samples, and radioactivity was measured in a liquid scintillation counter (TRI-CARB[®] 2260XL, Packard Instrument Inc.).

Plasma concentrations of liposomes (C_p) versus time curves were analyzed by the Eq. (1) using the non-linear least-squares regression program MULTI (Yamaoka et al., 1978).

$$C_p = A \cdot \exp(-\alpha \cdot t) + B \cdot \exp(-\beta \cdot t) \quad (1)$$

The area under the plasma concentration–time curve (AUC) was calculated by the following equation:

$$AUC_0^t = \int_0^t C_p dt \quad (2)$$

Total body clearance (CL_{total}), elimination rate constant (k_{el}), distribution volume of central compartment (Vd_c) and distribution volume at steady state (Vd_{ss}) were calculated by the following equations:

$$CL_{total} = \frac{Dose}{AUC_0^\infty} \quad (3)$$

$$Vd_c = \frac{Dose}{A + B} \quad (4)$$

$$k_{el} = \frac{CL_{total}}{Vd_c} \quad (5)$$

$$Vd_{ss} = \left(1 + \frac{k_{12}}{k_{21}} \cdot Vd_c\right) \quad (6)$$

where AUC_0^∞ means AUC value from 0 to infinity. k_{12} and k_{21} are first-order rate constants from peripheral to central compartment and from central to peripheral compartment, respectively. Tissue uptake clearance (CL_{tissue}) was calculated by the following equation:

$$CL_{tissue} = \frac{X_{tissue}^t}{AUC_0^t} \quad (t = 360 \text{ min}) \quad (7)$$

where AUC_0^t means AUC value from 0 to time t and X_{tissue}^t represents the amount of liposomes in a tissue at time t .

2.7. Single-pass liver perfusion experiments

Liver perfusion was carried out following the procedure reported previously (Furumoto et al., 2002). After the liver was stabilized by 13-min perfusion with Krebs–Ringer bicarbonate (KRB) buffer, each liposomal preparation was continuously infused at a concentration of 0.5 nmol total lipid/mL in the presence of 1% serum from the portal vein for 20 min. After 5-min wash with KRB buffer, the liver was excised, weighed and the accumulated amount of liposomes in the liver was evaluated by measuring the radioactivity in the liver as mentioned above. The serum was prepared just before use as follows: rat whole blood was collected from the carotid artery and allowed to clot at room temperature for 20 min, then centrifuged at $1500 \times g$ for 20 min at 4 °C and the supernatant obtained was used. To investigate the contribution of the receptor-mediated endocytosis to the uptake of liposomes, the perfused liver was pretreated with 10 µg/mL trypsin for 10 min (Ogawara et al., 1999).

2.8. Quantitative and qualitative determination of serum protein associated onto liposomal surface

Aliquots of 3H -liposomal suspension (2.5 µmol total lipid/mL) were incubated with equal volume of fresh rat serum for 20 min at 37 °C. Then, the liposomes were separated from bulk serum proteins by Sepharose CL-4B gel filtration (Johnstone et al., 2001). Fractions of liposomes were collected, and the amount of serum proteins associated on liposomes was quantified by Lowry's method (Lowry et al., 1951) and the amount of liposomes was quantified by measuring the radioactivity. SDS-polyacrylamide gel electrophoresis (SDS-PAGE) was performed by using the Mini Protean-II electrophoretic apparatus (Bio-Rad, Hercules, CA, USA) on 12.5% polyacrylamide gel (Ready Gel J, Bio-Rad). For the relative comparison of the proteins associated on the surface of each liposomal

preparation, the same amount of protein (0.3 µg) was loaded onto the gel. The detection of proteins was performed by a silver-stain procedure by using a silver-stain kit (Daiichi Pure Chemicals, Tokyo).

After SDS-PAGE was performed as described above, proteins were blotted on cellulose nitrate membrane (Advantec, Tokyo). For the detection of complement C3 or IgG, the blots were incubated with 1:100 diluted goat anti-rat complement C3 or 1:250 diluted rabbit anti-rat IgG polyclonal antibody. As second antibodies, peroxidase-linked anti-goat polyclonal antibody (Cosmo Bio, Tokyo) and anti-rabbit polyclonal antibody (Zymed® laboratories Inc., CA, USA) were used at 1:10,000 and 1:5000 dilution in blocking buffer, respectively. The protein band was visualized with the enhanced chemiluminescence (ECL) system (Amersham Pharmacia Biotech, Buckinghamshire, UK) and the densitometric intensities of protein bands were quantified by Scion Image™ (Scion Corporation, Frederick, MD). Since SDS-PAGE was conducted under reducing condition where many small fragments can be generated from the protein of interest, the densitometric intensities of bands were integrated for each lane to semi-quantitatively evaluate the amount of C3 and IgG.

2.9. Sample preparation for LC-MS/MS analysis and data search

The protein bands were excised from the gel and transferred to Ependorf tubes. The gel pieces were washed twice with 50% acetonitrile/25 mM ammonium bicarbonate, washed with 100% acetonitrile and then dried in a speed vacuum concentration system (CVE-100D, Rikakikai, Tokyo). Approximately 30 µL of trypsin (20 µg/mL) in 25 mM ammonium bicarbonate was added to the dried residue and the samples were incubated overnight at 37 °C. The supernatant was transferred to a separate Ependorf tube and the peptides were further extracted from the gel pieces by incubation in 50% acetonitrile/5% formic acid (FA) for about 4 h at room temperature. The supernatants obtained from the two steps were pooled, dried by SpeedVac and dissolved in 5 µL 50% acetonitrile/0.1% FA and stored at –20 °C until use. Sample analysis was performed on Agilent 1100LC/MSD Trap XCT series system. The ionization system was Chip Cube using HPLC-Chip-Ms (Agilent Technologies, Santa Clara, CA, USA). The chip was automatically loaded and positioned into the MS nanospray chamber. The chip contained a Zobrax 300SB-C₁₈ (43 mm × 75 µm, 5 µm) column and a Zobrax 300SB-C₁₈ (40 nL, 5 µm) enrichment column. The mobile phase, the mixture of H₂O/0.1% FA and acetonitrile/10% H₂O/0.1% FA, was delivered at the flow rate of 300 nL/min. Tryptic peptides were eluted from the column into the MS using gradient elution. The capillary voltage was set to 1850 V, the flow and temperature of the drying gas were 4 L/min and 300 °C, respectively. The MS and MS/MS data were analyzed by Data Analysis software (Spectrum Mill Ver. 3.3).

2.10. Statistical analysis

Results are expressed as the mean ± S.D. Analysis of variance (ANOVA) was used to test the statistical significance of differences among groups. Statistical significance in the differences of the means was evaluated by using Student's *t*-test or Tukey's test for the single or multiple comparisons of experimental groups, respectively.

3. Results and discussion

In order to prolong the residence time of liposomes in the systemic circulation, PVA as well as PEG were employed to modify the surface of liposomes. In this study, we prepared five different

Table 1
Composition and physical properties of liposomes

Liposomes	Liposomes composition EPC:Chol:PEG:PVA (molar ratio)	Particle size (nm)	Zeta potential (mV)
Naked	60:40:0:0	90.8 ± 0.9	-29.0 ± 1.2
PEG5%	55:40:5:0	88.5 ± 1.2	-4.5 ± 0.8*
PEG4%/PVA1%	55:40:4:1	91.1 ± 2.1	3.7 ± 0.5*
PEG1%/PVA4%	55:40:1:4	124.2 ± 2.2*	0.7 ± 0.8*
PVA5%	55:40:0:5	141.0 ± 0.6*	0.4 ± 1.0*

Results for particle size and zeta potential are expressed as the mean ± S.D. of three experiments.

* $p < 0.05$, compared with naked liposome.

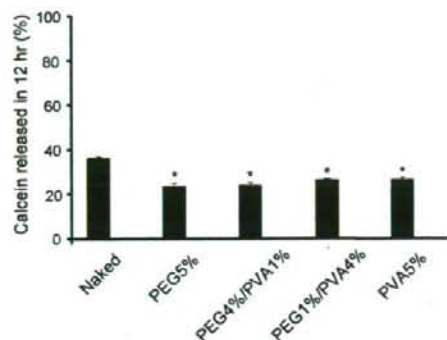


Fig. 1. In vitro release of calcein from surface-modified liposomal preparations. Each liposomal preparation was incubated in PBS (pH 7.4) containing 10% rat serum (v/v) at 37 °C for 12 h. Results are expressed as the mean with the vertical bar showing S.D. of three experiments. * $p < 0.05$, compared with naked liposome.

liposomal preparations including naked liposome, PEG liposome (PEG5%), liposomes modified with the mixture of both PEG and PVA (PEG4%/PVA1% and PEG1%/PVA4%) and liposome modified with PVA only (PVA5%). It is well known that PEG-DSPE is stably inserted into the lipid bilayer of liposomes (Parr et al., 1994). The 1-h incubation with 50% rat serum at 37 °C revealed that more than 90% of PVA incorporated stably remained on the liposomes, suggesting that the hydrophobic moiety of PVA derivative was also stably inserted into the lipid bilayer of liposomes as suggested by Takeuchi et al. (1998).

Since several factors such as particle size, charge and lipid composition have been reported to influence the in vivo fate of liposomes after intravenous administrations (Levchenko et al., 2002; Murao et al., 2002; Awasthi et al., 2003), the physicochemical properties of the liposomes prepared were examined (Table 1). The particle sizes for naked and PEG liposomes were found to be almost the same, while the modification of liposomes with PVA increased the particle size depending on its molar ratio. The measurement of zeta potential showed that the negative charge of naked liposome tended to be neutralized by the surface-modification either

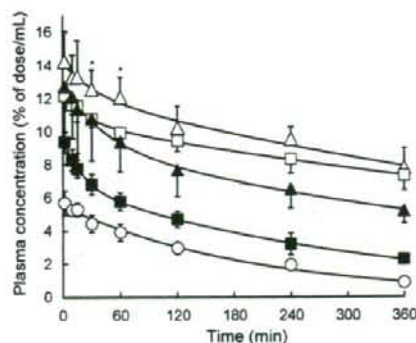


Fig. 2. Plasma concentration–time profile of surface-modified liposomal preparations after intravenous injection into rats. Each liposomal preparation was injected at a dose of 10 μmol total lipid/kg. Results are expressed as the mean with the vertical bar showing S.D. of three rats. Keys: ○, Naked; □, PEG5%; △, PEG4%/PVA1%; ▲, PEG1%/PVA4%; ■, PVA5%. * $p < 0.05$ compared with PEG5% liposome.

with PEG, PVA or their mixture. In order to confirm the stability of prepared liposomes in the presence of serum, calcein release from each liposomal preparation was determined. As illustrated in Fig. 1, the surface-modified liposomes were characterized by the significant lower release of calcein compared to the naked liposome, demonstrating their good stability in the presence of serum.

In vivo pharmacokinetics and biodistribution of the surface-modified liposomes were investigated after intravenous administration to rats. Fig. 2 shows the plasma concentration–time profiles of the liposomes, and the pharmacokinetic parameters obtained are summarized in Table 2. As shown in Fig. 2, naked liposome was rapidly eliminated from systemic circulation with the largest values of k_{el} , V_d and V_{dss} (Table 2). On the other hand, other polymer-modified liposomes exhibited longer blood circulating properties. Among them, PEG4%/PVA1% liposome showed the smallest Cl_{total} and the largest $AUC_{0-\infty}$, which was about 12 times or 1.2 times larger than that of naked liposome or PEG5% liposome, respectively (Table 2). In addition, the PEG4%/PVA1% liposome showed significantly higher plasma levels than PEG5% liposome at 30 and 60 min after intravenous injection. Moreover, the PEG4%/PVA1% liposome provided the smallest values of both V_d and k_{el} among the liposomal preparations examined, where the small V_d and k_{el} would mean the decrease in the rapid distribution to the liver just after dosing and the delay of elimination from plasma, respectively. Tissue uptake clearances calculated for various organs would support the above consideration (Fig. 3). The hepatic clearances for the liposomes modified with polymers were significantly smaller than that for naked liposome, and PEG4%/PVA1% liposome provided the smallest value of hepatic clearance among the liposomes investigated. Furthermore, it is worth to note that PEG4%/PVA1% liposome showed significantly smaller clearances for liver (68%), spleen (38%) and lung (22% of PEG5%) than PEG5% liposome. On the other hand,

Table 2
Pharmacokinetic parameters of different liposomal formulations after intravenous injection into rats

Parameters	Naked	PEG5%	PEG4%/PVA1%	PEG1%/PVA4%	PVA5%
AUC (% of dose min/mL)	1096 ± 101	10755 ± 3012 ^{**}	13438 ± 4520 ^{**}	6045 ± 604	2267 ± 282
Cl_{total} (μL/min)	91.9 ± 8.3	9.7 ± 2.4 ^{**}	8.0 ± 2.4 ^{**}	16.7 ± 1.6 ^{**}	44.6 ± 5.3 ^{**}
k_{el} (min ⁻¹)	4.98 ± 0.24	1.21 ± 0.36 ^{**}	1.13 ± 0.36 ^{**}	2.12 ± 0.25 ^{**}	4.29 ± 0.42
V_d (mL)	18.4 ± 1.1	8.1 ± 0.5 ^{**}	7.1 ± 0.9 ^{**}	8.0 ± 1.7 ^{**}	10.4 ± 0.7
V_{dss} (mL)	18.4 ± 1.1	9.4 ± 0.3 ^{**}	9.5 ± 2.3 ^{**}	10.6 ± 2.3 ^{**}	14.3 ± 1.4

Each pharmacokinetic parameter was obtained by following the equations described in Section 2. Results are expressed as the mean ± S.D. of three rats.

** $p < 0.01$, compared with naked liposome.

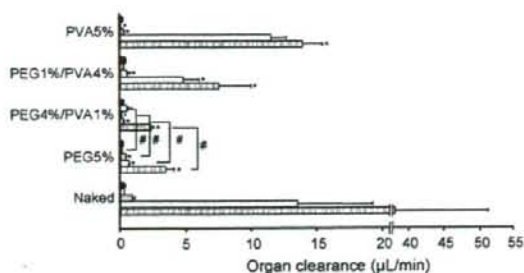


Fig. 3. Tissue uptake clearances of surface-modified liposomes after intravenous injection into rats. Each liposomal preparation was injected at a dose of $10 \mu\text{mol}$ total lipid/kg. Each tissue was excised at 6 h after injection. Results are expressed as the mean with the vertical bar showing S.D. of three rats. Keys: \blacksquare , liver; \square , spleen; \blacksquare , lung; \square , kidney; \blacksquare , heart. $^{\#} p < 0.05$ compared with naked liposome; $^* p < 0.05$ compared with PEG5% liposome.

the renal uptake clearance was larger for PEG4%/PVA1% liposome than that for PEG5% liposome. The reason for it remains to be clarified, but the longer circulation of larger amount of liposomes might lead to the disposition of intact and/or degraded liposomes into kidney.

To clarify the mechanism behind the less affinity of PEG4%/PVA1% than PEG5% to the liver where these liposomes were mainly distributed, a single-pass liver perfusion experiment was performed by using the perfusate containing 1% serum (v/v) (Fig. 4). Naked liposome showed significantly higher hepatic accumulation ($4.3 \pm 1.2 \text{ nmol}$ total lipid) than the two polymer-modified liposomes. In addition, the hepatic accumulation of PEG4%/PVA1% liposome ($0.6 \pm 0.2 \text{ nmol}$ total lipid) was significantly lower than PEG5% ($1.9 \pm 0.3 \text{ nmol}$ total lipid). These results were similar to those obtained in the in vivo study (Figs. 2 and 3 and Table 2). Furthermore, the pretreatment of the perfused liver with trypsin drastically decreased the hepatic accumulation of both naked ($0.96 \pm 0.1 \text{ nmol}$ total lipid) and PEG5% liposomes ($0.90 \pm 0.06 \text{ nmol}$ total lipid). On the contrary, the same treatment did not significantly affect the hepatic accumulation of PEG4%/PVA1% liposome ($0.70 \pm 0.20 \text{ nmol}$ total lipid). These results clearly indicate that the modification of liposomes with the mixture of PEG4%/PVA1% can avoid the hepatic disposition via the receptor-mediated endocytosis, which, on the other hand, substantially contributes to the hepatic disposition of PEG5% liposome.

It is well known that the hepatic uptake of liposomes is largely affected by the association of serum opsonins such as IgG,

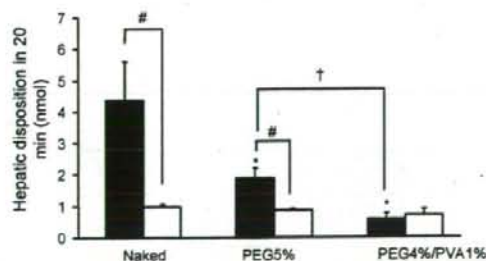


Fig. 4. Hepatic disposition of naked, PEG5% and PEG4%/PVA1% liposomes in single-pass liver perfusion experiments. The liver perfusion was performed for 20 min. Results are expressed as the mean with the vertical bar showing S.D. of three experiments. Keys: \blacksquare , control; \square , + trypsin treatment. $^{\#} p < 0.05$, compared with naked, control or PEG5% liposome, respectively.

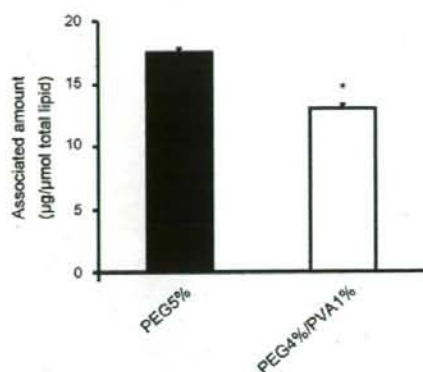


Fig. 5. Amount of serum proteins associated on the surface of PEG5% and PEG4%/PVA1% liposomes. Results are expressed as the mean with the vertical bar showing S.D. of three experiments. $^{\#} p < 0.05$, compared with PEG5% liposome.

fibrinectin, complement components, C-reactive protein and α_2 -macroglobulin (Tsujimoto et al., 1981; Rossi and Wallace, 1983; Bonte and Juliano, 1986; Huong et al., 2001; Price et al., 2001; Ishida et al., 2006; Moghimi et al., 2006). In addition, the recognition of surface-bound opsonins by their corresponding receptors is known to be a main trigger for the hepatic uptake of particles via receptor-mediated endocytosis (Moghimi and Davis, 1994; Liu et al., 1995). Therefore, we tried to evaluate the serum proteins associated on the surface of PEG5% liposome and PEG4%/PVA1% liposome quantitatively and qualitatively. As illustrated in Fig. 5, the total amount of serum proteins adsorbed on the surface of the PEG4%/PVA1% liposome ($13.0 \pm 0.3 \mu\text{g}/\mu\text{mol}$ total lipid) was significantly smaller than that for PEG5% liposome ($18.0 \pm 0.4 \mu\text{g}/\mu\text{mol}$ total lipid). This result was in good agreement with the previous report demonstrating that the circulation half-lives of liposomes after intravenous administration is inversely related to the total protein amount associated on the surface (Chonn et al., 1992). It has previously been reported that the fixed aqueous layer thickness (FALT) around liposomes was increased by the surface-modification with PEG and that thicker FALT would be likely to prevent serum proteins from interacting with liposomes (Shimada et al., 1995; Zeisig et al., 1996). Moreover, it has been postulated that surface-grafted PEG would form either a mushroom or a brush conformation, depending on molecular weight and surface density of PEG on the liposomes, and that the latter conformation would build the thicker FALT than the former one (Needham et al., 1997; Nicholas et al., 2000; Johnstone et al., 2001). Sadzuka et al. (2002) reported that the surface-modification with the mixture of PEG500 and PEG2000 provided thicker FALT than the modification with either PEG500 or PEG2000, and that the liposomes modified with both PEG500 and PEG2000 revealed the lowest hepatic uptake. They speculated that PEG500 would facilitate to transform of PEG2000 from the mushroom structure into the brush one, and that the liposomes on which less amount of opsonins would be adsorbed due to thicker FALT had lower affinity to the liver (Sadzuka et al., 2002). Considering this background, we speculated that PVA alone on the surface of liposomes would be present as the mushroom (shrunk) structure with thin FALT. Then, further addition of adequate amount of PEG might facilitate the conformational change of PVA to the brush-like (extended) structure with thicker FALT, leading to the decrease in the adsorbed amount of serum proteins on PEG4%/PVA1% liposome. In the case of PEG1%/PVA4% liposome, the amount of PEG might be still insufficient to facilitate the conformational change of PVA. Sadzuka et

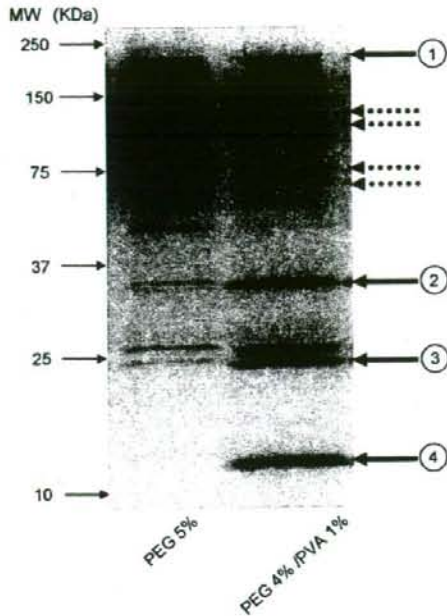


Fig. 6. Comparison of serum proteins associated on the surface of PEG5% and PEG4%/PVA1% liposomes. The same amount of protein (0.3 μ g) was loaded onto each lane. SDS-PAGE was performed following the procedure described in Section 2, and proteins were silver-stained. Solid and dotted arrows indicate the typical proteins increased and decreased on PEG4%/PVA1% liposome, respectively, as compared with PEG5% liposome.

al. (2002) proposed that the optimal amount of PEG500 would be needed to support the brush-like structure of PEG2000 and it could also be the case with PEG/PVA liposomes. To have better understanding of the mechanisms; however, the conformational dynamics of PVA molecule on the surface have to be elucidated and will be the subject of our further study.

In order to identify the proteins adsorbed on the liposomes, SDS-PAGE was at first performed. The results revealed that there was quite large difference in the profiles of surface-associated serum proteins between PEG5% liposome and PEG4%/PVA1% liposome (Fig. 6). The proteins highlighted with dotted arrows seem to be preferentially associated onto PEG5% liposome. On the other hand, the proteins highlighted with solid arrows (15, 25, 35 and 240 kDa) are associated more onto PEG4%/PVA1% liposome. Taken the results obtained in the *in vivo* and liver perfusion studies together, the proteins with dotted arrows might contain opsonins enhancing the hepatic uptake of PEG5% liposome, while the proteins with solid arrows might possess dysopsonin-like activity suppressing the uptake of PEG4%/PVA1% liposome.

As discussed above, complement C3 (C3) and IgG are the major opsonins and are known to play important roles to promote the hepatic uptake of liposomes via their corresponding receptors expressed on the surface of Kupffer cells in the liver (Ishida et al., 2002). Therefore, we conducted the Western blot analysis to compare the amounts of C3 and IgG associated on the surface of PEG5% and PEG4%/PVA1% liposomes (Fig. 7). As shown in Fig. 7A and B, the semi-quantification of the densitometric intensities derived from C3 and IgG fragments revealed that these typical opsonins associated more with PEG5% liposome than PEG4%/PVA1% liposome.

Besides opsonins, it has been suggested that there are some dysopsonins in serum, which can inhibit phagocytosis of pathogens or particles. Although it was reported that immunoglobulin A and α_1 -acid glycoprotein functioned as dysopsonins for microorganisms (Van Oss et al., 1974; Absolom, 1986), there is no identified serum components with dysopsonic activity for liposomes so far. Then, we tried to identify the proteins which might act as dysopsonin for PEG4%/PVA1%, highlighted with solid arrows in Fig. 6. After SDS-PAGE was performed for proteins associated on PEG4%/PVA1% liposome, the proteins highlighted with solid arrows in Fig. 6 were subjected to LC-MS/MS system for identification and the results were summarized in Table 3. The analysis showed that albumin would be one of the serum proteins preferentially associated onto PEG4%/PVA1% liposome. Taken our previous reports that the pre-coating of polystyrene nanospheres with albumin or the coupling of albumin onto the surface of PEG liposome reduced their affinity to the liver (Ogawara et al., 2004; Furumoto et al., 2007), albumin might function as dysopsonin for PEG4%/PVA1% liposome.

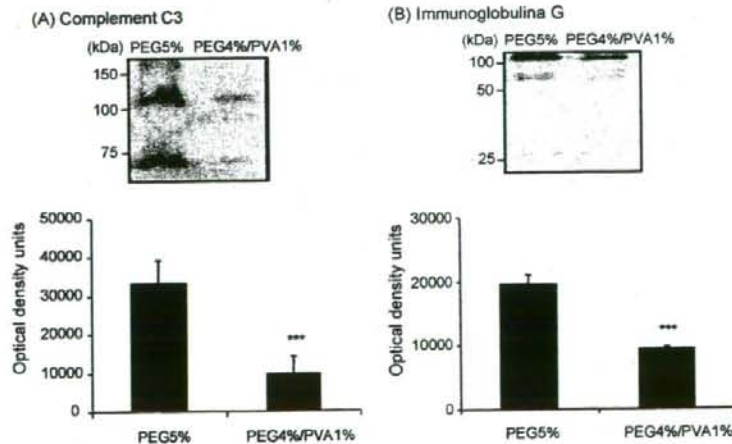


Fig. 7. Semi-quantification of complement C3 and immunoglobulin G associated on the surface of PEG5% and PEG4%/PVA1% liposomes by Western blot analysis. The same amount of protein (1.2 μ g) was loaded onto each lane. Results of semi-quantification are expressed as the mean with the bar showing S.D. of five experiments. *** $p < 0.05$ compared with PEG5% liposomes.

Table 3
Identification of several serum proteins associated on PEG4%/PVA1% liposome at larger amount than PEG5% liposomes

Band number	Identified proteins	Accession number	Spectrum Mill score
1	Apolipoprotein B	61098031	43.67
2	Apolipoprotein A-IV Albumin	8392909 55391508	96.62 41.07
3	Apolipoprotein E	37805241	186.39
4	Apolipoprotein A-I Albumin	113997	97.65

LC-MS/MS data were analyzed by Spectrum Mill with NCBInr database (<http://www.ncbi.nlm.nih.gov/>). The following filters were used after database searching: peptide score > 6, peptide% SPI > 60 and protein score > 11. Band numbers represent the proteins highlighted with solid arrows in Fig. 6.

In addition, apo A-I, A-IV, B and E were also shown to preferentially be associated onto PEG4%/PVA1% liposome. Although apoE itself is known to function as an opsonin for the uptake of particles by hepatocytes, Bisgaier et al. (1989) indicated that the co-existence of apoE with apoA-I, A-IV or B leads to the conformational change of apoE and abolishes its ability to enhance the uptake of liposomes by HepG2 cells. Therefore, the enrichment of these apolipoproteins on the surface of PEG4%/PVA1% liposome might abolish the opsonic activity of apoE. However, the mechanisms by which the specific proteins such as albumin, apo A-I, A-IV, B and E were preferentially associated onto PEG4%/PVA1% liposome are still unclear and would be investigated in the further study.

4. Conclusion

An incorporation of small percentage of PVA into PEG liposome (PEG4%/PVA1% liposome) improved the in vivo disposition characteristics, which could be attributed to lower hepatic distribution of PEG4%/PVA1% liposome. The decrease in the affinity to the liver would be attributed to lower amount of serum proteins including opsonins and larger amount of dysopsonins such as albumin adsorbed on the surface. These findings can form a solid basis to develop useful particulate drug carriers with better in vivo disposition characteristics. To confirm the advantage of PEG4%/PVA1% liposome, the in vivo anti-tumor activity of the liposome including some anti-tumor drug will be investigated in our next study.

References

Absolom, D.R., 1986. Opsonins and dysopsonins: an overview. *Methods Enzymol.* 132, 281–318.

Allen, T.M., Chonn, A., 1987. Large unilamellar liposomes with low uptake into the reticuloendothelial system. *FEBS Lett.* 223, 42–46.

Allen, T.M., Hansen, C., 1991. Pharmacokinetics of stealth versus conventional liposomes: effect of dose. *Biochim. Biophys. Acta* 1068, 133–141.

Allen, T.M., Hansen, C., Martin, F., Redemann, C., Yau-Young, A., 1991. Liposomes containing synthetic lipid derivatives of poly(ethylene glycol) show prolonged circulation half-lives in vivo. *Biochim. Biophys. Acta* 1066, 29–36.

Awasthi, V.D., Garcia, D., Goins, B.A., Phillips, W.T., 2003. Circulation and biodistribution profiles of long-circulating PEG-liposomes of various sizes in rabbits. *Int. J. Pharm.* 253, 121–132.

Banerjee, R., 2001. Liposomes: applications in medicine. *J. Biomater. Appl.* 16, 3–21.

Bisgaier, C.L., Siebenkas, M.V., Williams, K.J., 1989. Effects of apolipoproteins A-IV and A-I on the uptake of phospholipid liposomes by hepatocytes. *J. Biol. Chem.* 264, 862–866.

Bonte, F., Juliano, R.L., 1986. Interactions of liposomes with serum proteins. *Chem. Phys. Lipids* 40, 359–372.

Chonn, A., Semple, S.C., Cullis, P.R., 1992. Association of blood proteins with large unilamellar liposomes in vivo: relation to circulation lifetimes. *J. Biol. Chem.* 267, 18759–18765.

Furumoto, K., Ogawara, K., Nagayama, S., Takakura, Y., Hashida, M., Higaki, K., Kimura, T., 2002. Important role of serum proteins associated on the surface of particles in their hepatic disposition. *J. Control. Rel.* 83, 89–96.

Furumoto, K., Yokoe, J., Ogawara, K., Amano, S., Takaguchi, M., Higaki, K., Kai, T., Kimura, T., 2007. Effect of coupling of albumin onto surface of PEG liposome on its in vivo disposition. *Int. J. Pharm.* 329, 110–116.

Gabizon, A., Papahadjopoulos, D., 1988. Liposome formulations with prolonged circulation time in blood and enhanced uptake by tumors. *Proc. Natl. Acad. Sci. U.S.A.* 85, 6949–6953.

Huog, T.M., Ishida, T., Harashima, H., Kiwada, H., 2001. Species difference in correlation between in vivo/in vitro liposome-complement interactions. *Biol. Pharm. Bull.* 24, 439–441.

Ishida, T., Harashima, H., Kiwada, H., 2002. Liposome clearance. *Biosci. Rep.* 22, 197–224.

Ishida, T., Ichihara, M., Wang, X., Yamamoto, K., Kimura, J., Majima, E., Kiwada, H., 2006. Injection of PEGylated liposomes in rats elicits PEG-specific IgM, which is responsible for rapid elimination of a second dose of PEGylated liposomes. *J. Control. Rel.* 112, 15–25.

Johnstone, S.A., Masin, D., Mayer, L., Bally, M.B., 2001. Surface-associated serum proteins inhibit the uptake of phosphatidylserine and poly(ethylene glycol) liposomes by mouse macrophages. *Biochim. Biophys. Acta* 1513, 25–37.

Levchenko, T.S., Rammohan, R., Lukyanov, A.N., Whiteman, K.R., Torchilin, V.P., 2002. Liposome clearance in mice: the effect of a separate and combined presence of surface charge and polymer coating. *Int. J. Pharm.* 240, 95–102.

Lian, T., Ho, R., 2001. Trends and development in liposome drug delivery systems. *J. Pharm. Sci.* 90, 667–680.

Liu, D., Liu, F., Song, Y.K., 1995. Recognition and clearance of liposomes containing phosphatidylserine are mediated by serum opsonin. *Biochim. Biophys. Acta* 1235, 140–146.

Lowry, O.H., Rosebrough, N.J., Farr, A.L., Randall, R.J., 1951. Protein measurement with the Folin phenol reagent. *J. Biol. Chem.* 193, 265–275.

Maruyama, K., Ishida, O., Takizawa, T., Moribe, K., 1999. Possibility of active targeting to tumor tissues with liposomes. *Adv. Drug Deliv. Rev.* 40, 89–102.

Moghimi, S.M., Davis, S.S., 1994. Innovations in avoiding particle clearance from blood by Kupffer cells: cause for reflection. *Crit. Rev. Ther. Drug Carrier Syst.* 11, 31–59.

Moghimi, S.M., Hamad, I., Bunger, R., Andresen, T.L., Jorgensen, K., Hunter, A.C., Baranji, L., Rosivall, L., Szebeni, J., 2006. Activation of the human complement system by cholesterol-rich and PEGylated liposomes: modulation of cholesterol-rich liposome-mediated complement activation by elevated serum LDL and HDL levels. *J. Liposome Res.* 16, 167–174.

Murao, A., Nishikawa, M., Managit, C., Wong, J., Kawakami, S., Yamashita, F., Hashida, M., 2002. Targeting efficiency of galactosylated liposomes to hepatocytes in vivo: effect of lipid composition. *Pharm. Res.* 19, 1808–1814.

Needham, D., Stoiicheva, N., Zhelev, D.V., 1997. Exchange of monooleoylphosphatidylcholine as monomer and micelle with membranes containing poly(ethylene glycol)-lipid. *Bioophys. J.* 73, 2615–2629.

Nicholas, A.R., Scott, M.J., Kennedy, N.J., Jones, M.N., 2000. Effect of grafted polyethylene glycol (PEG) on the size, encapsulation efficiency and permeability of vesicles. *Biochim. Biophys. Acta* 1463, 167–178.

Ogawara, K., Furumoto, K., Nagayama, S., Minato, K., Higaki, K., Kai, T., Kimura, T., 2004. Pre-coating with serum albumin reduces receptor-mediated hepatic disposition of polystyrene nanoparticles: implications for rational design of nanoparticles. *J. Control. Rel.* 100, 451–455.

Ogawara, K., Yoshida, M., Takakura, Y., Hashida, M., Higaki, K., Kimura, T., 1999. Interaction of polystyrene microspheres with liver cells: role of membrane receptors and serum proteins. *Biochim. Biophys. Acta* 1472, 165–172.

Parr, M.J., Ansell, S.M., Choi, L.S., Cullis, P.R., 1994. Factors influencing the retention and chemical stability of poly(ethylene glycol)-lipid conjugates incorporated into large unilamellar vesicles. *Biochim. Biophys. Acta* 1195, 21–30.

Poste, G., Bucana, C., Raz, A., Bugelski, P., Kirsh, R., Fidler, I.J., 1982. Analysis of the fate of systemically administered liposomes and implications for their use in drug delivery. *Cancer Res.* 42, 1412–1422.

Price, M.E., Cornelius, R.M., Brash, J.L., 2001. Protein adsorption to polyethylene glycol modified liposomes from fibrinogen solution and from plasma. *Biochim. Biophys. Acta* 1512, 191–205.

Rossi, J.D., Wallace, B.A., 1983. Binding of fibrinectin to phospholipid vesicles. *J. Biol. Chem.* 258, 3327–3331.

Sadzuka, Y., Nakade, A., Hiram, R., Miyagishima, A., Nozawa, Y., Hirota, S., Sonobe, T., 2002. Effect of mixed polyethyleneglycol modification on fixed aqueous layer thickness and antitumor activity of doxorubicin containing liposome. *Int. J. Pharm.* 238, 171–180.

Senior, J.H., 1987. Fate and behavior of liposomes in vivo: a review of controlling factors. *Crit. Rev. Ther. Drug Carrier Syst.* 3, 123–193.

Shimada, K., Miyagishima, A., Sadzuka, Y., Nozawa, Y., Mochizuki, Y., Ohshima, H., Hirota, S., 1995. Determination of the thickness of the fixed aqueous layer around polyethyleneglycol-coated liposomes. *J. Drug Target* 3, 283–289.

Sihorkar, V., Vyas, S.P., 2001. Potential of polysaccharide anchored liposomes in drug delivery, targeting and immunization. *J. Pharm. Pharm. Sci.* 4, 138–158.

Stein, Y., Halperin, G., Stein, O., 1980. Biological stability of [³H] cholesteryl oleyl ether in cultured fibroblasts and intact rat. *FEBS Lett.* 111, 104–106.

Takeuchi, H., Kojima, H., Yamamoto, H., Kawashima, Y., 2000. Polymer coating of liposomes with a modified polyvinyl alcohol and their systemic circulation and RES uptake in rats. *J. Control. Rel.* 68, 195–205.

Takeuchi, H., Kojima, H., Yamamoto, H., Kawashima, Y., 2001. Evaluation of circulation profiles of liposomes coated with hydrophilic polymers having different molecular weights in rats. *J. Control. Rel.* 75, 83–91.

Takeuchi, H., Yamamoto, H., Toyoda, T., Toyobuku, H., Hino, T., Kawashima, Y., 1998. Physical stability of size controlled small unilamellar liposomes coated with a modified polyvinyl alcohol. *Int. J. Pharm.* 164, 103–111.

- Torchilin, V.P., 2005. Recent advances with liposomes as pharmaceutical carriers. *Nat. Rev. Drug Discov.* 4, 145–160.
- Tsujimoto, M., Inoue, K., Nojima, S., 1981. Reactivity of human C-reactive protein with positively charged liposomes. *J. Biochem. (Tokyo)* 90, 1507–1514.
- Van Oss, C.J., Gillman, C.F., Bronson, P.M., Border, J.R., 1974. Phagocytosis-inhibiting properties of human serum alpha-1 acid glycoprotein. *Immunol. Commun.* 3, 321–328.
- Yamaoka, K., Nakagawa, T., Uno, T., 1978. Statistical moments in pharmacokinetics. *J. Pharmacokinet. Biopharm.* 6, 547–558.
- Zeisig, R., Shimada, K., Hirota, S., Arndt, D., 1996. Effect of sterical stabilization on macrophage uptake in vitro and on thickness of the fixed aqueous layer of liposomes made from alkylphosphocholines. *Biochim. Biophys. Acta* 1285, 237–245.

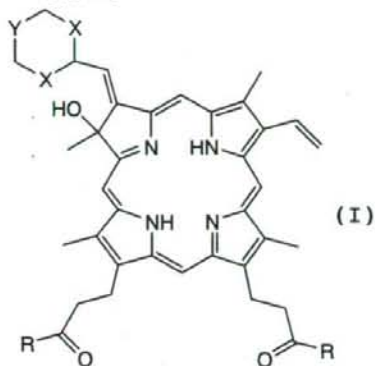
発明の名称 : 皮膚疾患治療剤
 出願番号 : 特願2008-118187
 出願日 : 2008年(平成20年)4月30日

【書類名】 特許請求の範囲

【請求項1】

次式(I) :

【化1】



(式中、

Xは、O又はSを表し、

Yは、 $-(CH_2)_n-$ 又は $-(CHOH)-$ を表し、

Rは、 $-OH$ 、 $-O(CH_2)_mCH_3-$ 、 $-O(CH_2)_l-OH$ 又は $-S(CH_2)_l-SH$ を表し、

nは、0~10の整数を表し、

mは、0~11の整数を表し、

lは、2~12の整数を表す)

で示されるクロリン誘導体又はその薬理的に許容される塩を有効成分とする光線力学療法(PDT: Photodynamic Therapy)用の皮膚疾患治療用剤。

【請求項2】

式(I)で示されるクロリン誘導体又はその薬理的に許容される塩を製剤重量に対して0.1~20.0重量%含有してなる請求項1に記載の光線力学療法(PDT)用の皮膚疾患治療用軟膏剤。

【請求項3】

軟膏基剤が、FAPG(H)軟膏基剤、FAPG(K)軟膏基剤、PEG軟膏基剤、PEG-PG軟膏基剤、ワセリン軟膏基剤、SRワセリン軟膏基剤、SRワセリン-IPM軟膏基剤またはプラスチック軟膏基剤から選択させるものである請求項4に記載の光線力学療法(PDT)用の皮膚疾患治療用軟膏剤。

Provided for non-commercial research and education use.
Not for reproduction, distribution or commercial use.



Volume 49, Issue 2, February 2008

ISSN 0923-1811

JOURNAL OF
DERMATOLOGICAL
SCIENCE



The official journal of
The Japanese Society for
Investigative Dermatology

Available online at
ScienceDirect
www.elsevier.com/locate/jds

This article was published in an Elsevier journal. The attached copy is furnished to the author for non-commercial research and education use, including for instruction at the author's institution, sharing with colleagues and providing to institution administration.

Other uses, including reproduction and distribution, or selling or licensing copies, or posting to personal, institutional or third party websites are prohibited.

In most cases authors are permitted to post their version of the article (e.g. in Word or Tex form) to their personal website or institutional repository. Authors requiring further information regarding Elsevier's archiving and manuscript policies are encouraged to visit:

<http://www.elsevier.com/copyright>



LETTER TO THE EDITOR

ATX-S10(Na)-photodynamic therapy inhibits cytokine secretion and proliferation of lymphocytes

KEYWORDS

ATX-S10(Na); HuT102 cells; IFN- γ ; IL-6; IL-8; TNF- α

Photodynamic therapy (PDT) is a new therapeutic modality for a variety of neoplasms, including skin tumors, lymphomas, as well as scleroderma. Now PDT using 5-aminolevulinic acid (ALA) is available for skin diseases and its effects on cytokine production have also been reported [1,2]. ATX-S10(Na), 13,17-bis(1-carboxypropionyl)carbamoylethyl-8-ethenyl-2-hydroxy-3-hydroxyiminoethylidene-2,7,12,18-tetramethylporphyrin sodium salt, is a new hydrophilic chlorine photosensitizer characterized by good accumulation in tumors [3,4], and rapid elimination in urine within 24–48 h. Thus ATX-S10(Na) is regarded as a good candidate for the second generation photosensitizer of PDT. Recent study from our laboratory has demonstrated that ATX-S10(Na)-PDT is effective for various skin tumors [5].

Psoriasis is a chronic inflammatory skin disease with hyperproliferative epidermis. It is assumed that T cells and various T cell-derived cytokines reveal an essential role on induction and maintenance of the psoriatic lesion [6]. In fact cyclosporine and various biological agents are effective for psoriasis. There are no reports, however, which describe the effect of PDT on cytokine production or T cell proliferation. In the present study, we investigated the effect of ATX-S10(Na)-PDT on the production of cytokines and viability of various T cell lines.

These cell lines include HuT102, MT-2, Jurkat, MoLT4, which are derived from mycosis fungoides, adult T cell leukemia, acute lymphoblastic leukemia,

and acute lymphoblastic leukemia, respectively. These were generous gifts from Dr. Hiroya Kobayashi (Pathology, Asahikawa Medical College, Japan). The cells were cultured in RPMI 1640 medium containing 10% fetal calf serum, 100 u/ml penicillin, and 100 μ g/ml streptomycin at 37 °C in CO₂ in air. In order to determine the production of cytokines, 10⁶ cells were cultured for 24 h and supernatants were collected. Then various cytokines, TNF- α , IFN- γ , IL-2, IL-5, IL-6, and IL-8, were assayed using ELISA kits, which were purchased from BioSource International, Inc. (California, USA). In a preliminary study, HuT102 cells produced abundant cytokines, such as TNF- α , IFN- γ , IL-6, and IL-8, but not IL-2, or IL-5 (data not shown). Then we analyzed the effect of ATX-S10(Na)-PDT on the cytokine production of HuT102 cells.

HuT102 cells (1×10^6) were cultured in the presence of 10 μ g/ml ATX-S10(Na) for 3 h and the cells were washed with phosphate-buffered saline (PBS). Then the cells were irradiated with diode laser (LD670-05, Hamamatsu Photonics K.K, Hamamatsu, Japan). At the indicated time the supernatants were collected and cytokine assays were performed. ATX-S10(Na)-PDT significantly inhibited TNF- α , IFN- γ , IL-6, and IL-8 production and the maximal effect was observed at 24 h (Fig. 1). The effect was irradiation dose-dependent. ATX-S10(Na) or the laser irradiation alone did not affect the cytokine secretions or cell proliferation (data not shown). Similar inhibitory effects on the cytokines production were observed by ATX-S10(Na)-PDT using MT-2, Jurkat, and MoLT4 cells (data not shown).

The effect of ATX-S10(Na)-PDT on cell proliferation was performed by non-radioactive proliferation assay using tetrazolium as indicator (Promega, Madison, WI). Various doses of laser were irradiated on 1×10^6 HuT102 cells, which were pretreated by 10 μ g/ml ATX-S10(Na) for 3 h. The decrease in cell proliferation was observed at 6 h and the maximal effect was detected at 24 h (data not shown). The suppressive effect was detected at 40 mJ/cm² with dose-dependent inhibition up to 100 mJ/cm²

Abbreviations: PBS, phosphate-buffered saline; PDT, photodynamic therapy.